

Introduction to Nuclear Fusion as An Energy Source



Po-Yu Chang

Institute of Space and Plasma Sciences, National Cheng Kung University

Lecture 9

2024 spring semester

Wednesday 9:10-12:00

Materials:

<https://capst.ncku.edu.tw/PGS/index.php/teaching/>

Online courses:

<https://nckucc.webex.com/nckucc/j.php?MTID=ma76b50f97b1c6d72db61de9eaa9f0b27>

Course Outline



- **Magnetic confinement fusion (MCF)**
 - Gyro motion, MHD
 - 1D equilibrium (z pinch, theta pinch)
 - Drift: ExB drift, grad B drift, and curvature B drift
 - Tokamak, Stellarator (toroidal field, poloidal field)
 - Magnetic flux surface
 - 2D axisymmetric equilibrium of a torus plasma: Grad-Shafranov equation.
 - Stability (Kink instability, sausage instability, Safety factor Q)
 - Central-solenoid (CS) start-up (discharge) and current drive
 - CS-free current drive: electron cyclotron current drive, bootstrap current.
 - Auxiliary Heating: ECRH, Ohmic heating, Neutral beam injection.

Example of the analytical solution of the Grad-Shafranov equation



$$\Delta^* \psi = -\mu_0 R^2 \frac{dp}{d\psi} - \frac{1}{2} \frac{dF^2}{d\psi}$$

• For $\mu_0 \frac{dp}{d\psi} = -C_2$ $\frac{1}{2} \frac{dF^2}{d\psi} = C_1$

$$\psi(R, z) = -\frac{C_1}{2} z^2 + \frac{C_2}{8} R^4 + C_3 + C_4 R^2 + C_5 (R^4 - 4R^2 z^2)$$

$$C_1 = 1$$

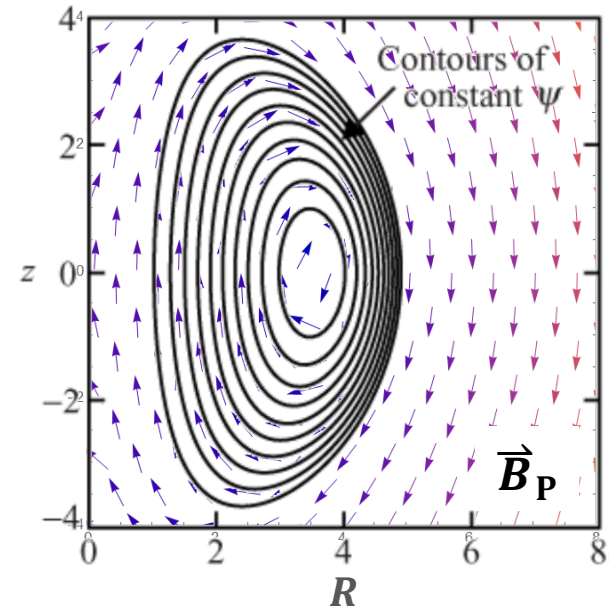
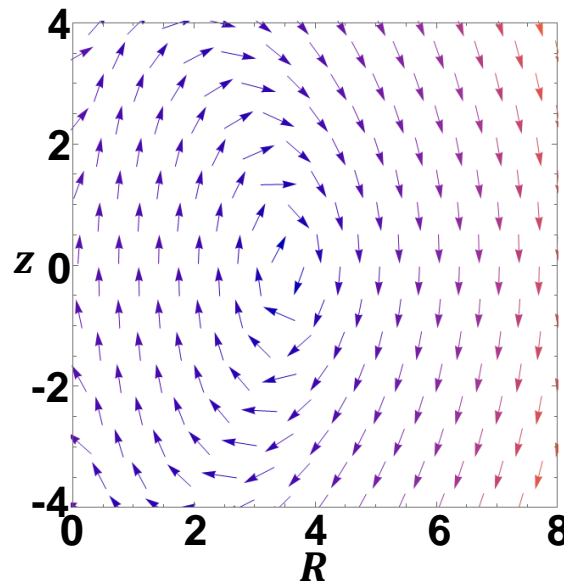
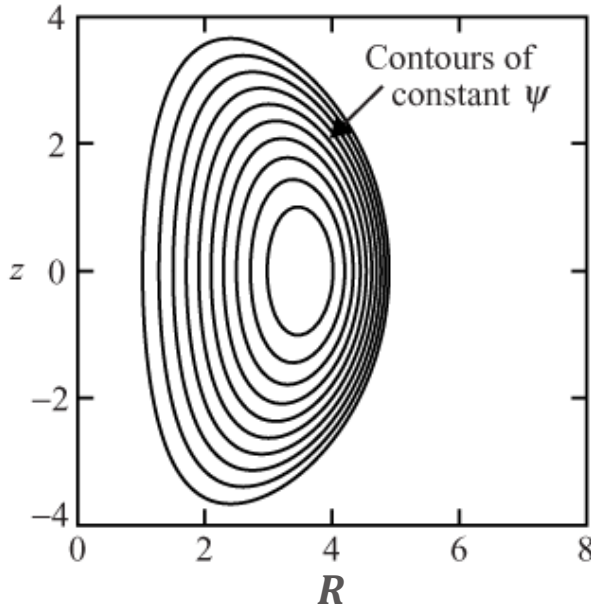
$$C_2 = -8$$

$$C_3 = -20$$

$$C_4 = 20$$

$$C_5 = 0.2$$

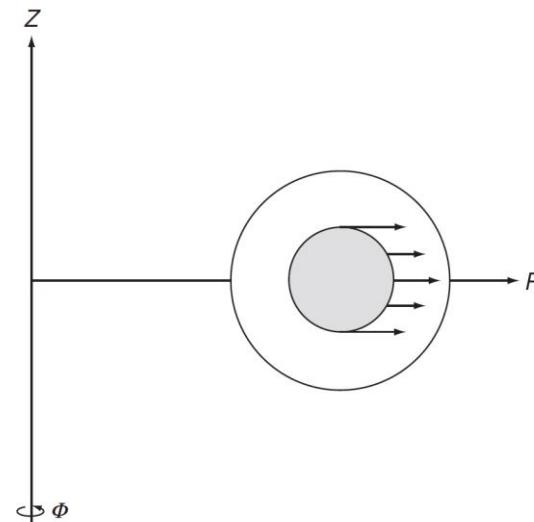
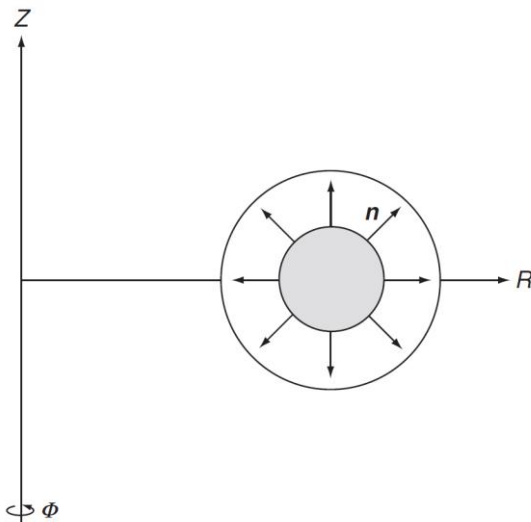
$$B_R(R, z) = -\frac{1}{R} (-C_1 z - 8C_5 R^2 z) \quad B_z(R, z) = \frac{1}{R} \left(\frac{C_2}{2} R^3 + 2C_4 R + C_5 (4R^3 - 8Rz^2) \right)$$



Magnetically confined toroidal equilibrium



1. Radial pressure balance in the poloidal plan needs to be provided so that the pressure contours form closed nested surfaces. Both toroidal and poloidal fields can readily accomplish this task.
 2. The radially outward expansion force inherent in all toroidal geometries needs to be balanced without sacrificing stability.
- Forces associated with toroidal force balance are usually than those corresponding to radial pressure balance. However, they are more difficult to compensate.



Toroidal configuration with a purely poloidal magnetic field

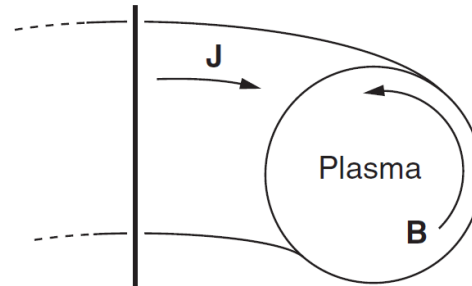
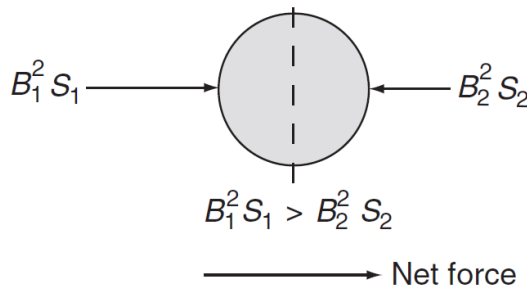
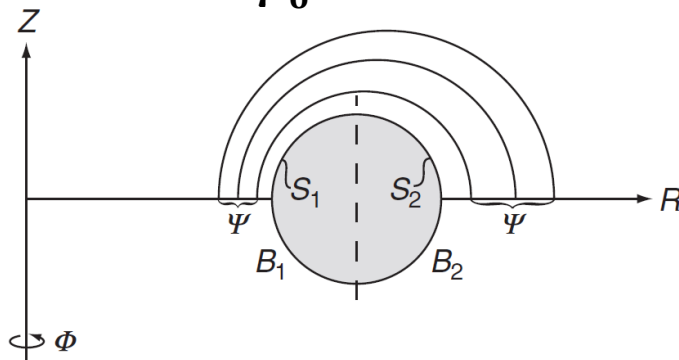


- Hoop force:

$$\psi_1 = \psi_2 \equiv \psi$$

$$S_1 < S_2 \quad B_1 > B_2$$

$$\vec{F}_{H,R} \propto \hat{e}_R \frac{B_1^2 S_1 - B_2^2 S_2}{2\mu_0} > 0$$

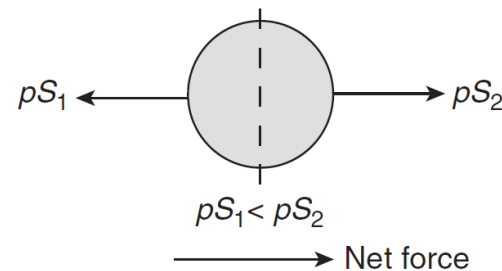
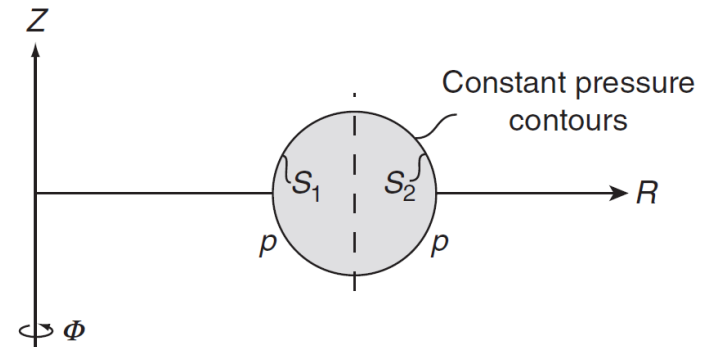


- Tire tube force

$$p_1 = p_2 \equiv p$$

$$S_1 < S_2$$

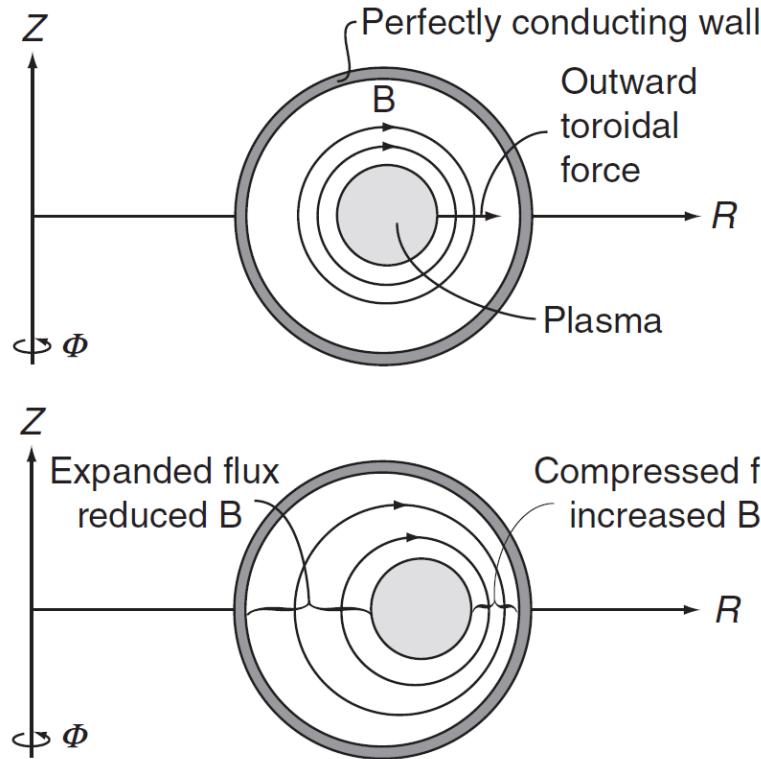
$$\vec{F}_{T,R} \propto -\hat{e}_R (pS_1 - pS_2) > 0$$



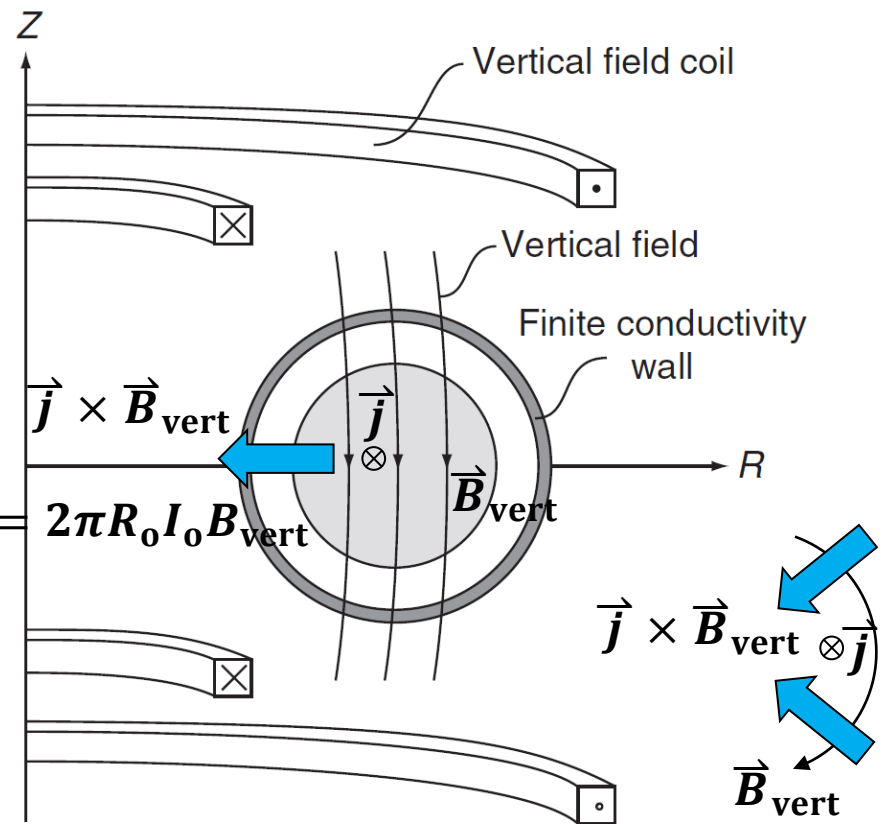
The outward force can be compensated by either a perfectly conducting shell or externally applied vertical field



- **Perfectly conducting shell**

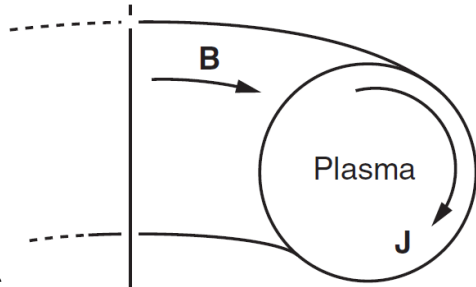


- **Externally applied vertical field**

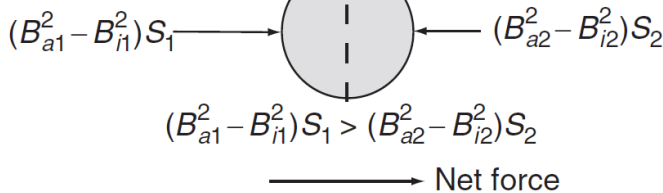
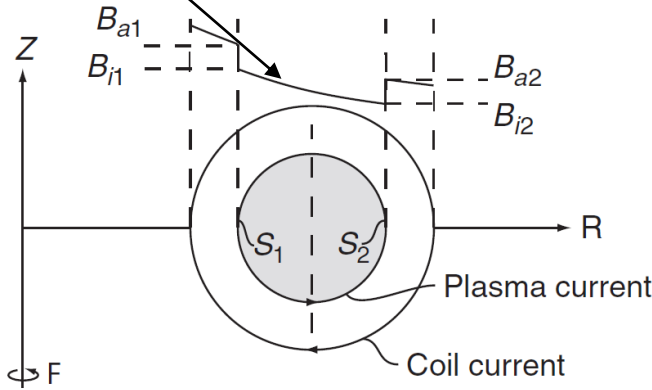


- **With a finite conductivity wall, flux can only remain compressed for about a skin time.**
- **This configuration develops disastrous MHD instabilities (z pinch).**

Toroidal configuration with a purely toroidal magnetic field, stable but NOT balanced

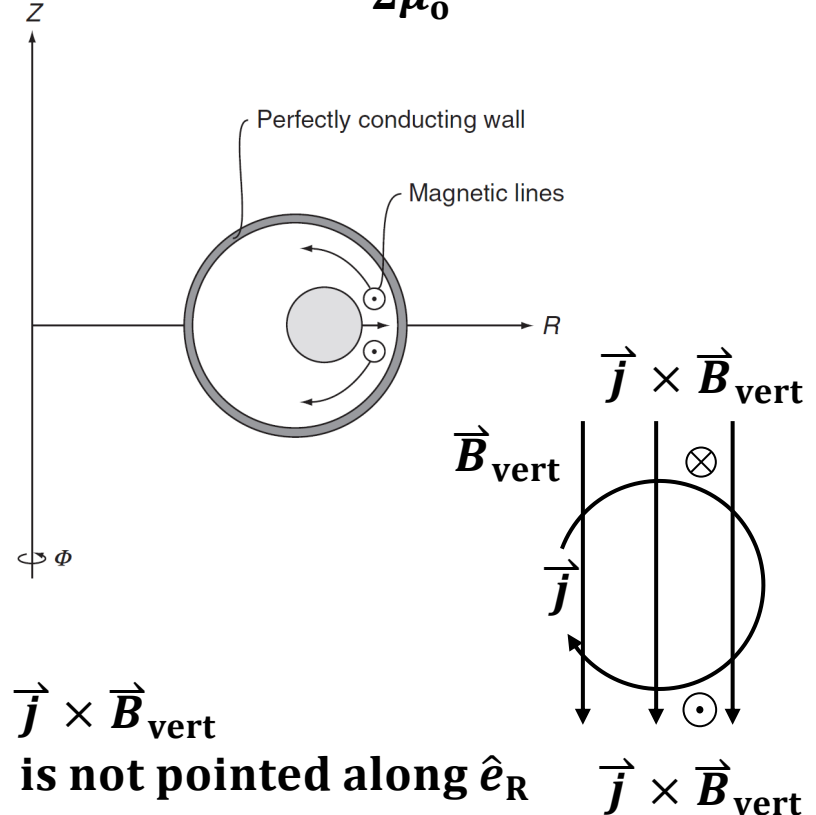


Plasma is diamagnetic

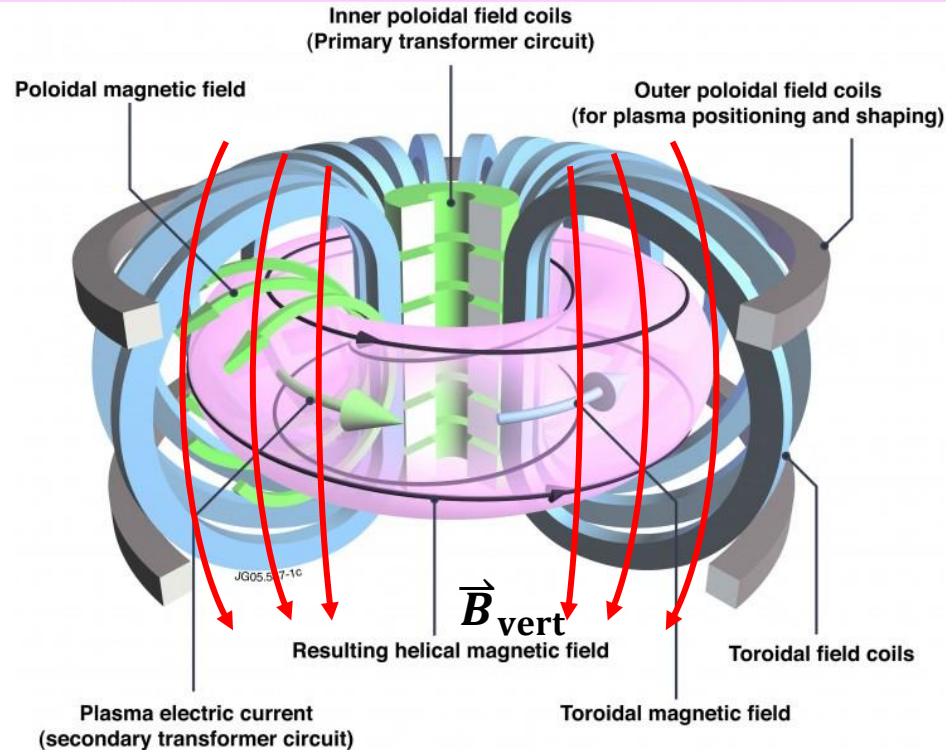


$$\vec{B} = B_\phi \hat{e}_\phi \quad B_\phi = B_0 \frac{R_0}{R} \quad B_0 = \frac{\mu_0 I_c}{2\pi R_0}$$

$$\vec{F}_R \propto \hat{e}_R \frac{(B_{a1}^2 - B_{i1}^2)S_1 - (B_{a2}^2 - B_{i2}^2)S_2}{2\mu_0} > 0$$



Coils in a tokamak



- **Toroidal field coils (in poloidal direction) – generate toroidal field for confinement.**
- **Poloidal field coils – generate vertical field for plasma positioning and shaping.**
- **Central solenoid – for breakdown and generating plasma current (in toroidal direction) and thus generating poloidal field for confinement.**

Plasma condition can be obtained by solving Grad-Shafranov equation



$$\Delta^* \psi = -\mu_0 R^2 \frac{dp}{d\psi} - \frac{1}{2} \frac{dF^2}{d\psi} \quad \text{where } \Delta^* \psi = R^2 \nabla \cdot \left(\frac{\nabla \psi}{R^2} \right)$$

- The usual strategy to solve the Grad-Shafranov equation:
 1. Specify two free functions, the plasma pressure $p = p(\psi)$ and the toroidal field function $F = F(\psi)$.
 2. Solve the equation with specified boundary conditions to determine the flux function $\psi(R, z)$.
 3. Calculation the magnetic field using the following equations:

$$B_R = -\frac{1}{R} \frac{\partial \psi}{\partial z} \quad B_\phi = \frac{F(\psi)}{R} \quad B_z = \frac{1}{R} \frac{\partial \psi}{\partial R}$$

4. The pressure profile can then be obtained from $p = p(\psi(R, z))$.

Application of solving Grad-Shafranov equation for designing a tokamak



- Given I_{plasma} , $p(\psi)$, $I(\psi)$, I_{coils} , free boundary of plasma, perfect conductor as the chamber.
- Given I_{plasma} , $p(\psi)$, $I(\psi)$, I_{coils} , free boundary of plasma, insulator chamber.
- Given I_{plasma} , $p(\psi)$, $I(\psi)$, I_{coils} , free boundary of plasma, chamber with eddy current.
- Given I_{plasma} , $p(\psi)$, $I(\psi)$, fixed boundary of plasma. Then, use I_{coils} , free boundary of plasma and match the plasma shape calculated in the fixed boundary condition.

$$\Delta^* \psi = -\mu_0 R^2 \frac{dp}{d\psi} - \frac{1}{2} \frac{dF^2}{d\psi} \quad \text{where } \Delta^* \psi = R^2 \nabla \cdot \left(\frac{\nabla \psi}{R^2} \right)$$

$$I_p = -2\pi F(\psi)$$

$$\mu_0 \vec{j} = \left(\frac{\nabla F}{R} \right) \times \hat{\phi} + \left(-\frac{1}{R} \Delta^* \psi \right) \hat{\phi} \quad \vec{B} = \left(\frac{\nabla \psi}{R} \right) \times \hat{\phi} + \frac{F(\psi)}{R} \hat{\phi}$$

Application of solving Grad-Shafranov equation for reconstructing a tokamak equilibrium state



- **Measure**

- boundary conditions, including ψ , B , etc., on the wall (using flux loop and B-dot probe).
- Pressure.
- Plasma current (using Rogowski coil).

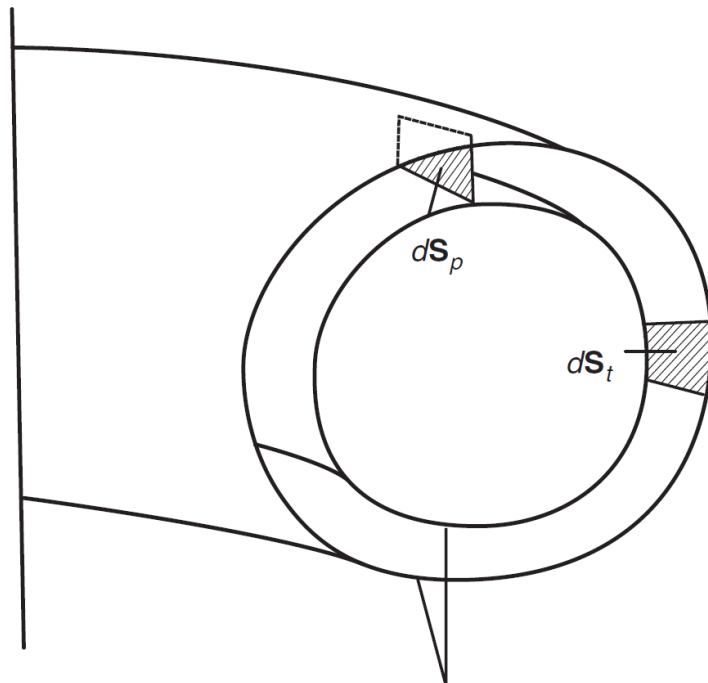
- Reconstruct $\psi(r,z)$, j , $p(\psi)$, $I(\psi)$, etc.

$$\Delta^* \psi = -\mu_0 R^2 \frac{dp}{d\psi} - \frac{1}{2} \frac{dF^2}{d\psi} \quad \text{where } \Delta^* \psi = R^2 \nabla \cdot \left(\frac{\nabla \psi}{R^2} \right)$$

$$I_p = -2\pi F(\psi)$$

$$\mu_0 \vec{j} = \left(\frac{\nabla F}{R} \right) \times \hat{\phi} + \left(-\frac{1}{R} \Delta^* \psi \right) \hat{\phi} \quad \vec{B} = \left(\frac{\nabla \psi}{R} \right) \times \hat{\phi} + \frac{F(\psi)}{R} \hat{\phi}$$

Fluxes and currents



Two neighboring flux surfaces

- **Poloidal flux:** $\psi_p = \int \vec{B} \cdot d\vec{S}_p$
 $\psi_p = \psi_p(p)$
- **Toroidal flux:** $\psi_t = \int \vec{B} \cdot d\vec{S}_t$
- **Poloidal current:** $I_p = \int \vec{j} \cdot d\vec{S}_p$
- **Toroidal current:** $I_t = \int \vec{j} \cdot d\vec{S}_t$

Normalized plasma pressure, β



$$\beta = \frac{\text{plasma pressure}}{\text{magnetic pressure}} = \frac{2\mu_0 \langle p \rangle}{B^2}$$

- Plasma pressure: $\langle p \rangle = \frac{1}{V_p} \int p d\vec{r}$

- Magnetic pressure: $P_B = \frac{B^2}{2\mu_0}$

$$B^2 = B_t^2 + B_p^2 = B_0^2 + \left(\frac{\mu_0 I_p}{2\pi a}\right)^2 \frac{2}{1 + \kappa^2}$$

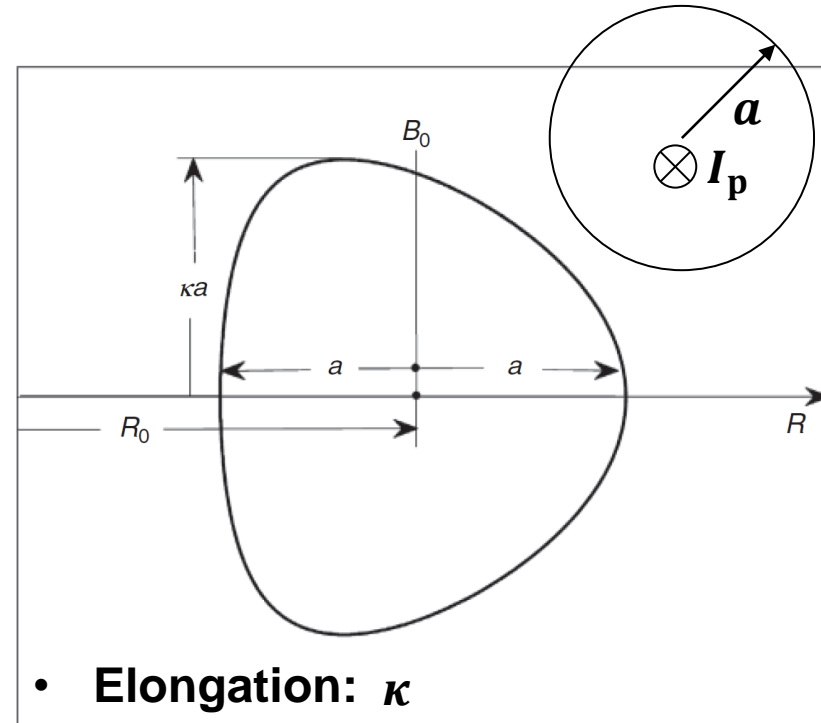
$$B_t^2 = B_0^2 \quad B_0 = B @ R = R_0$$

$$B_p^2 = \left(\frac{\mu_0 I_p}{2\pi a}\right)^2 = \left(\frac{\mu_0 I_p}{C_p}\right)^2$$

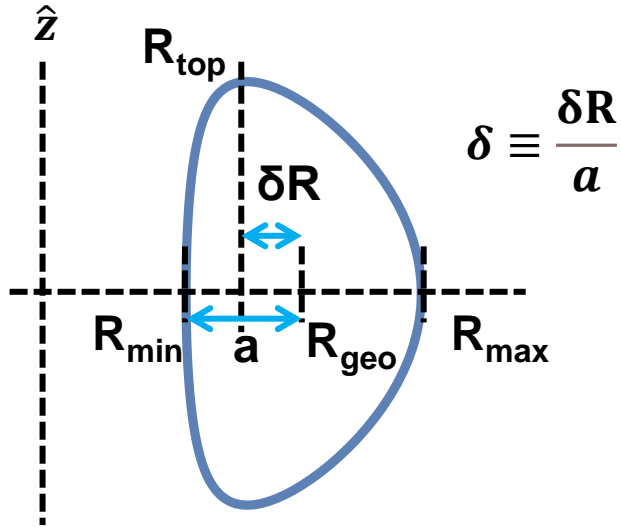
$$C_p \approx 2\pi a \sqrt{\frac{1 + \kappa^2}{2}}$$

$$\beta_t = \frac{2\mu_0 \langle p \rangle}{B_0^2} \quad \beta_p = \frac{4\pi^2 a^2 (1 + \kappa^2) p}{\mu_0 I_p^2}$$

$$\frac{1}{\beta} = \frac{1}{\beta_t} + \frac{1}{\beta_p}$$



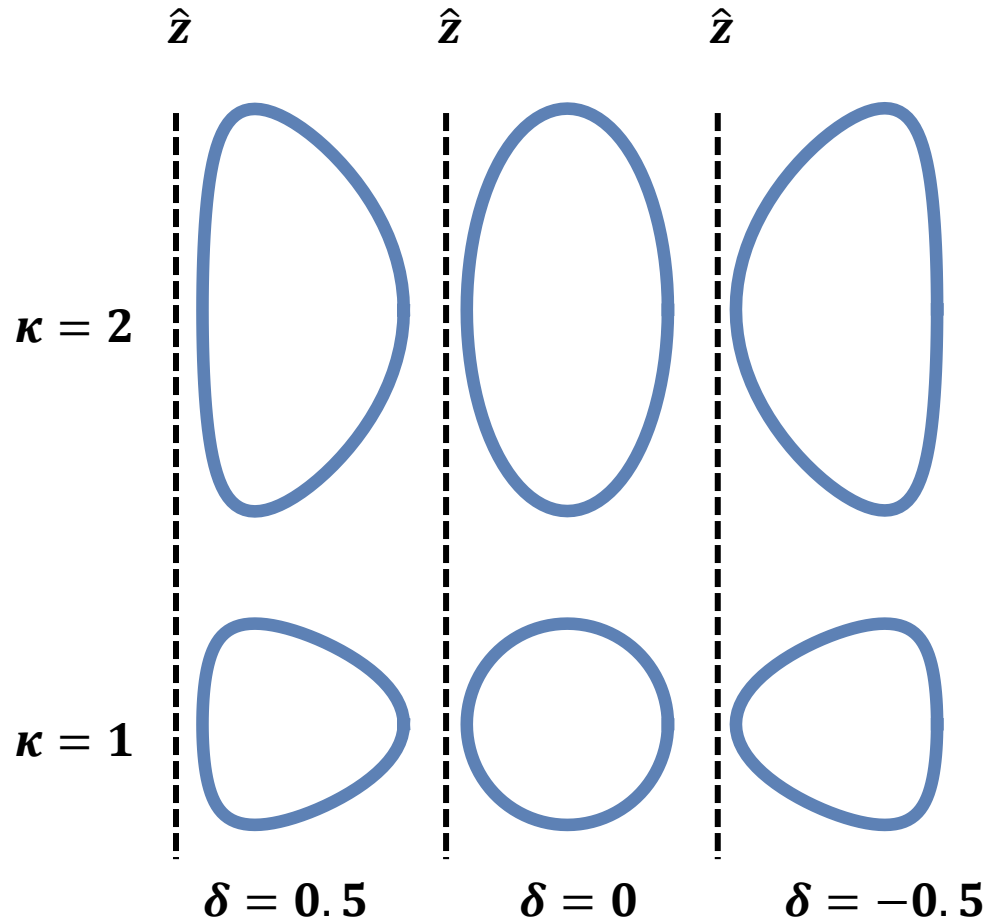
Different poloidal shapes



$$r = R + a \cos(\theta + \delta \sin(\theta))$$

$$z = a \kappa \sin(\theta)$$

- Aspect ratio: $\frac{R}{a}$
- Elongation: κ
- Triangularity: δ

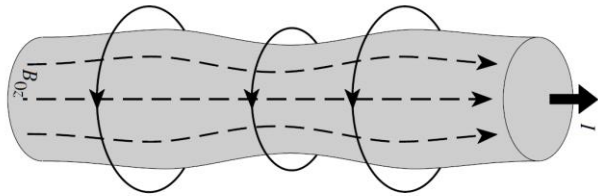


Safety factor

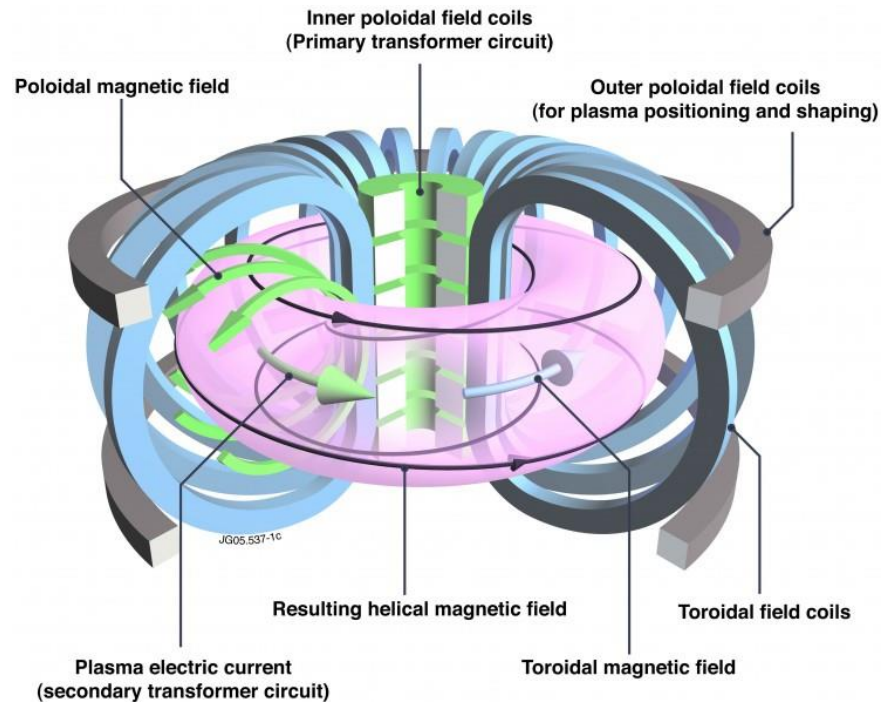


- Kink Safety Factor:

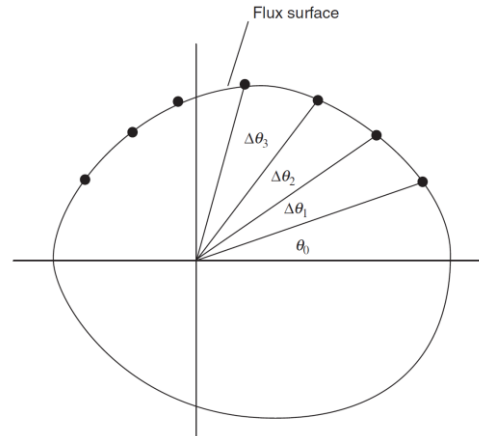
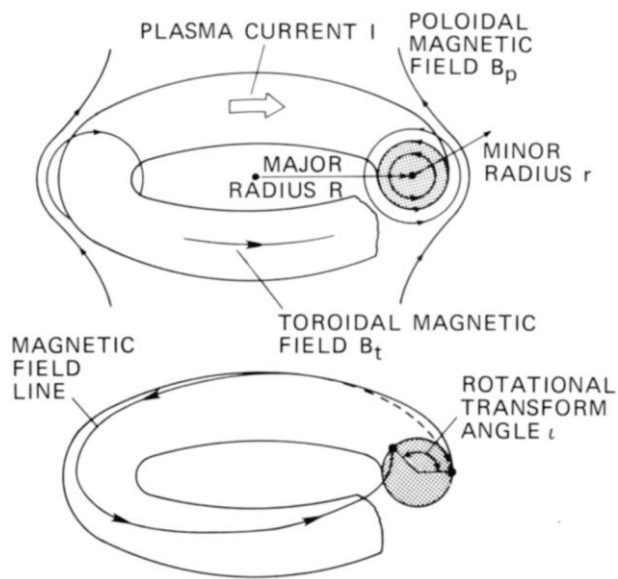
$$q^*(r) = \frac{aB_o}{R_oB_p} = \frac{2\pi a^2 \kappa B_o}{\mu_o R_o I_o}$$



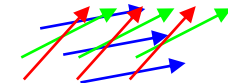
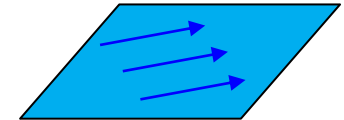
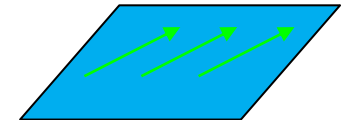
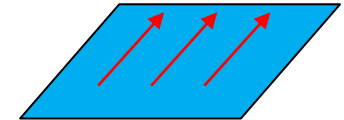
$$q(r) = \frac{rB_z(r)}{R_oB_\theta(r)}$$



Safety factor



- **Shear:**



- **Rotational transform:**
$$\iota \equiv \lim_{N \rightarrow \infty} \frac{1}{N} \sum \Delta\theta_n$$
- **MHD safety factor:**
$$q(V) \equiv \frac{2\pi}{\iota(V)} = \frac{d\psi_t/dV}{d\psi_p/dV}$$
 $\psi_t = \psi_t(V) \quad \psi_p = \psi_p(V)$
- **Shear:**
$$s(V) \equiv 2 \frac{V}{q} \frac{dq}{dV}$$

$$\iota(V) \equiv 2\pi \left(\frac{d\psi_p/dV}{d\psi_t/dV} \right)$$

Magnetic well



$$\widehat{W} = 2 \frac{V}{\langle B^2 \rangle} \frac{d}{dV} \left\langle \frac{B^2}{2} \right\rangle$$

$$= 2 \frac{V}{\langle B^2 \rangle} \frac{d}{dV} \left\langle \mu_0 p + \frac{B^2}{2} \right\rangle$$

- A magnetic well is a quantity that measures plasma stability against short perpendicular wavelength modes driven by the plasma pressure gradient.



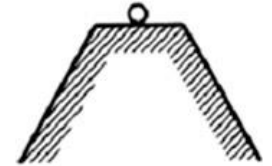
A

NO EQUILIBRIUM



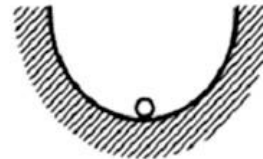
B

NEUTRALLY STABLE



C

(METASTABLE) EQUILIBRIUM



D

STABLE EQUILIBRIUM



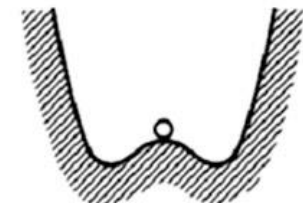
E

UNSTABLE EQUILIBRIUM



F

EQUILIBRIUM WITH LINEAR STABILITY AND NONLINEAR INSTABILITY



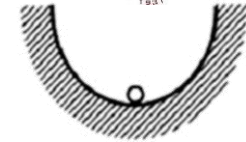
G

EQUILIBRIUM WITH LINEAR INSTABILITY AND NONLINEAR STABILITY

Variational formulation for checking stabilization



- **Equilibrium state:** $\vec{j}_o \times \vec{B}_o = \nabla p_o$
 - **Momentum eq:** $\rho_m \left[\frac{\partial \vec{v}}{\partial t} + (\vec{v} \cdot \nabla) \vec{v} \right] = \vec{j} \times \vec{B} - \nabla \cdot \vec{P}$
- $$\rho_m = \rho_o + \tilde{\rho}_1 \quad p = p_o + \tilde{p}_1 \quad \vec{v} = \vec{v}_o + \vec{v}_1 = \vec{v}_1 \equiv \frac{\partial \vec{\xi}}{\partial t}$$
- $$\vec{j} = \vec{j}_o + \vec{j}_1 \quad \vec{B} = \vec{B}_o + \vec{B}_1 \equiv \vec{B}_o + \vec{Q}$$



D

STABLE EQUILIBRIUM



E

UNSTABLE EQUILIBRIUM

$$\rho_m \frac{\partial^2 \vec{\xi}}{\partial t^2} = \vec{F}(\vec{\xi}) \quad \vec{F}(\vec{\xi}) = \vec{j}_o \times \vec{Q} + \vec{j}_1 \times \vec{B}_o - \nabla \tilde{p}_1$$

$$\vec{F}(\vec{\xi}) = \frac{1}{\mu_o} (\nabla \times \vec{B}_o) \times \vec{Q} + \frac{1}{\mu_o} (\nabla \times \vec{Q}) \times \vec{B}_o + \nabla (\vec{\xi} \cdot \nabla p + \gamma p \nabla \cdot \vec{\xi})$$

- **The change in potential energy associated with the perturbation:**

$$\delta W = -\frac{1}{2} \int \vec{\xi}^* \cdot \vec{F}(\vec{\xi}) d\vec{r} \quad \bullet \quad \text{Stable requirement: } \delta W \geq 0$$

$$\delta W_F = \frac{1}{2} \int d\vec{r} \left[\frac{|\vec{Q}_\perp|^2}{\mu_o} + \frac{B^2}{\mu_o} |\nabla \cdot \vec{\xi}_\perp + 2 \vec{\xi}_\perp \cdot \vec{\kappa}|^2 + \gamma p |\nabla \cdot \vec{\xi}|^2 \right. \\ \left. - 2(\vec{\xi}_\perp \cdot \nabla p) (\vec{\kappa} \cdot \vec{\xi}_\perp^*) - J_\parallel (\vec{\xi}_\perp^* \times \vec{b}) \cdot \vec{Q}_\perp \right]$$

Variational formulation for checking stabilization

- The change in potential energy associated with the perturbation:

$$\delta W = -\frac{1}{2} \int \vec{\xi}^* \cdot \vec{F}(\vec{\xi}) d\vec{r} \quad \bullet \text{ Stable requirement: } \delta W \geq 0$$

$$\delta W_F = \frac{1}{2} \int d\vec{r} \left[\frac{|\vec{Q}_\perp|^2}{\mu_0} + \frac{B^2}{\mu_0} |\nabla \cdot \vec{\xi}_\perp + 2 \vec{\xi}_\perp \cdot \vec{\kappa}|^2 + \gamma p |\nabla \cdot \vec{\xi}|^2 - 2(\vec{\xi}_\perp \cdot \nabla p)(\vec{\kappa} \cdot \vec{\xi}_\perp^*) - J_\parallel (\vec{\xi}_\perp^* \times \vec{b}) \cdot \vec{Q}_\perp \right]$$

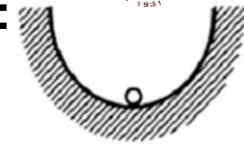
- Stabilization terms:

$$\frac{|\vec{Q}_\perp|^2}{\mu_0}: \text{ For bending magnetic field lines, (shear Alfvén wave).}$$

$$\frac{B^2}{\mu_0} (|\nabla \cdot \vec{\xi}_\perp + 2 \vec{\xi}_\perp \cdot \vec{\kappa}|)^2: \text{ For compressing the magnetic field, (compressional Alfvén wave).}$$

$$\gamma p |\nabla \cdot \vec{\xi}|^2: \text{ For compressing the plasma, (sound wave).}$$

- Destabilization terms: $-2(\vec{\xi}_\perp \cdot \nabla p)(\vec{\kappa} \cdot \vec{\xi}_\perp^*) - J_\parallel (\vec{\xi}_\perp^* \times \vec{b}) \cdot \vec{Q}_\perp$



D

STABLE EQUILIBRIUM



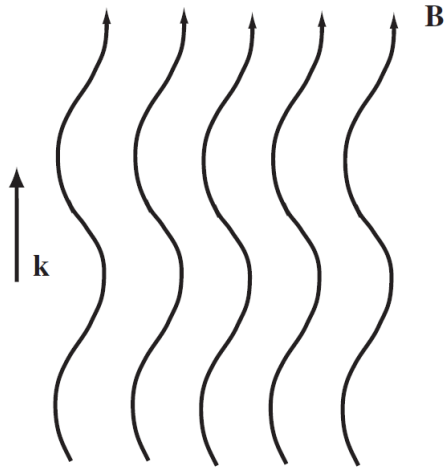
E

UNSTABLE EQUILIBRIUM

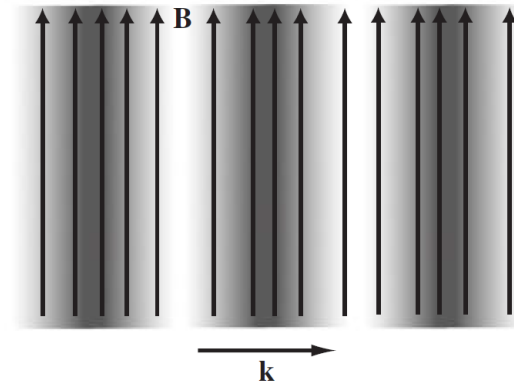
Alfvén waves



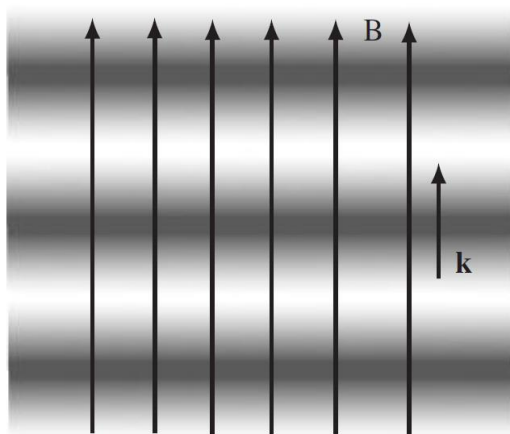
- Shear Alfvén wave:



- The fast magnetosonic wave (Compressional Alfvén wave):



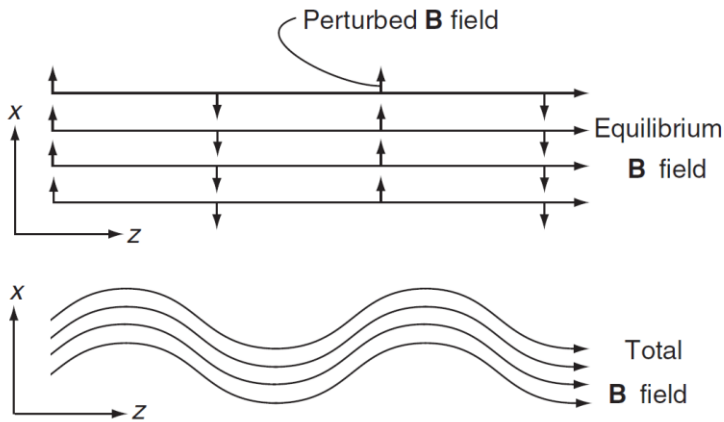
- Longitudinal sound wave (the slow magnetosonic wave)



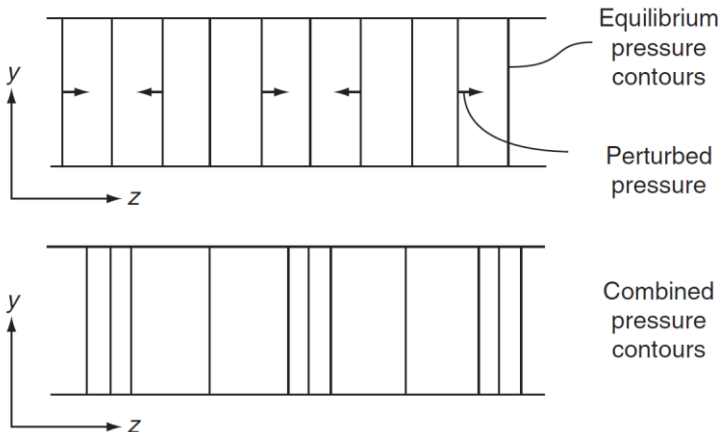
Alfvén waves



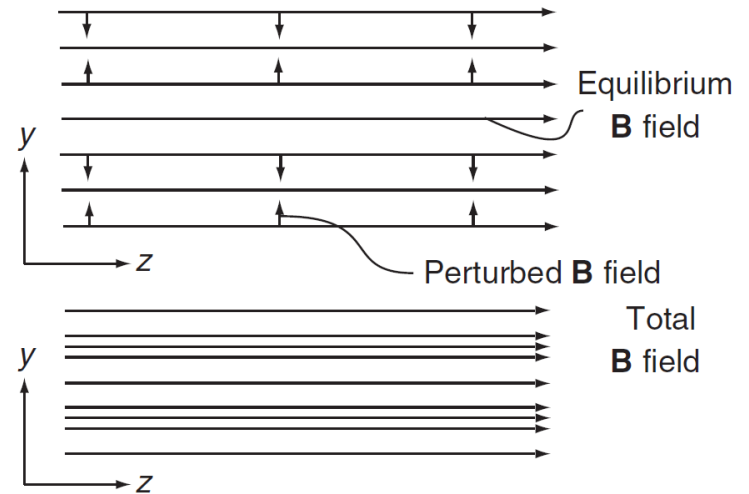
- **Shear Alfvén wave:**



- **The slow magnetosonic wave (Shear + Compressional Alfvén wave):**



- **The fast magnetosonic wave (Compressional Alfvén wave):**



Classification of MHD instabilities



- **Locations:**
 - **Internal/Fixed boundary modes:** mode structure does not require any motion of the plasma-vacuum interface away from its equilibrium position.
 - **External/Free-boundary modes:** the plasma-vacuum interface moves from its equilibrium position during an unstable MHD perturbation.
- **Dominant destabilizing term**
 - **Pressure-driven modes:** the dominant destabilizing term is the one proportional to ∇p .
 - **Current-driven modes:** the dominant destabilizing term is the one proportional to J_{\parallel} .

$$\delta W_F = \frac{1}{2} \int d\vec{r} \left[\frac{|\vec{Q}_{\perp}|^2}{\mu_0} + \frac{B^2}{\mu_0} |\nabla \cdot \vec{\xi}_{\perp} + 2 \vec{\xi}_{\perp} \cdot \vec{\kappa}|^2 + \gamma p |\nabla \cdot \vec{\xi}|^2 - 2(\vec{\xi}_{\perp} \cdot \nabla p) (\vec{\kappa} \cdot \vec{\xi}_{\perp}^*) - J_{\parallel} (\vec{\xi}_{\perp}^* \times \vec{b}) \cdot \vec{Q}_{\perp} \right]$$

Classification of MHD instabilities

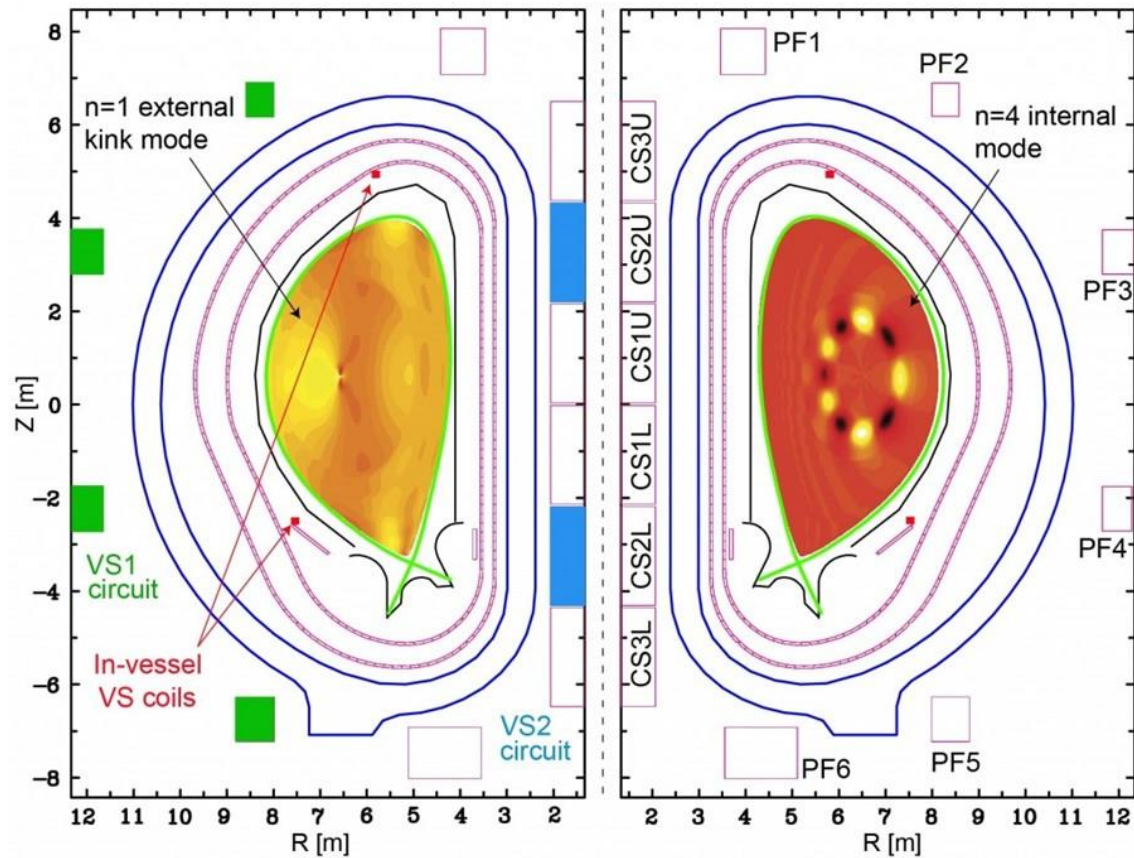


- **Locations:**
 - **Internal/Fixed boundary modes:** mode structure does not require any motion of the plasma-vacuum interface away from its equilibrium position.
 - **External/Free-boundary modes:** the plasma-vacuum interface moves from its equilibrium position during an unstable MHD perturbation.
- **Dominant destabilizing term**
 - **Current-driven modes, e.g., kink instability, sausage instability.**
 - **Pressure-driven modes, e.g., interchange mode, ballooning mode.**

External mode vs internal mode



- Predicted behaviors of the plasma in ITER

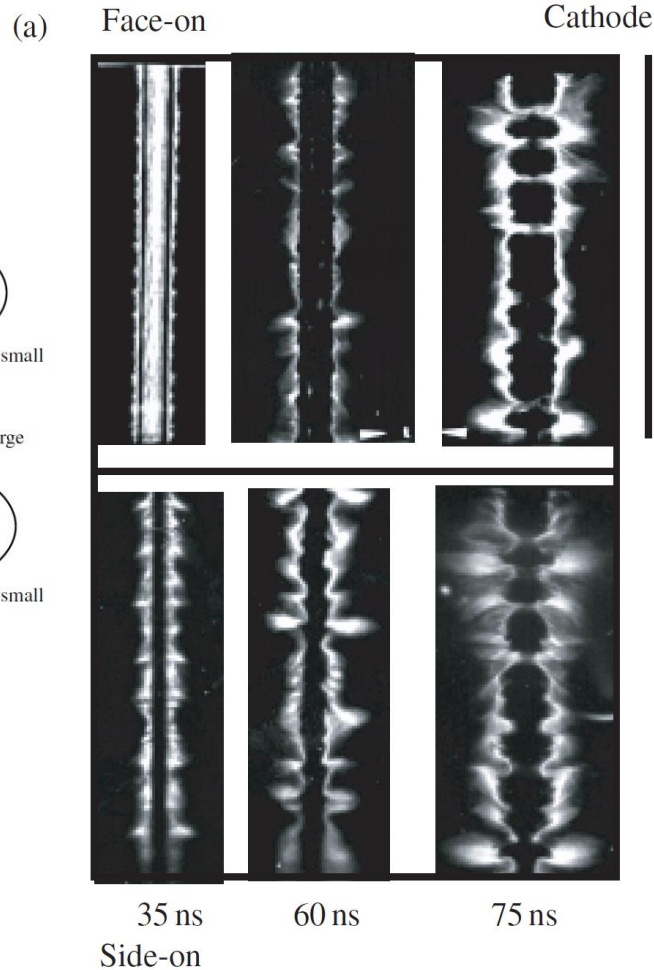


Current-driven instability



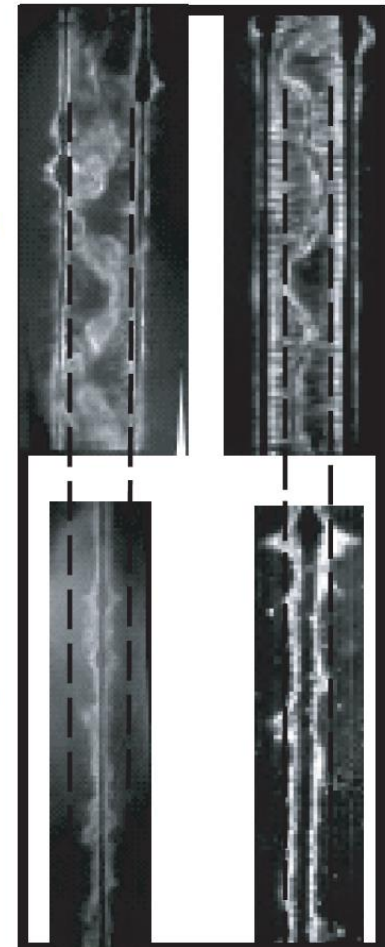
- Sausage instability ($m=0$)

- Kink instability ($m=1$)

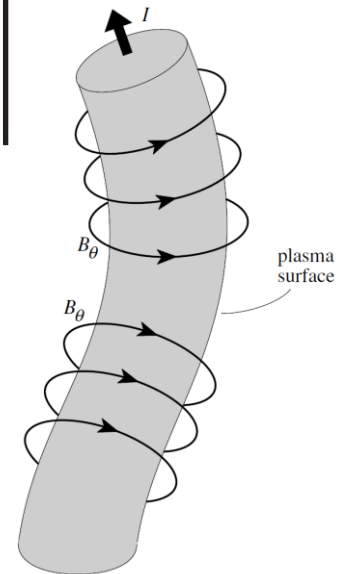


8.3 mm
Face-on

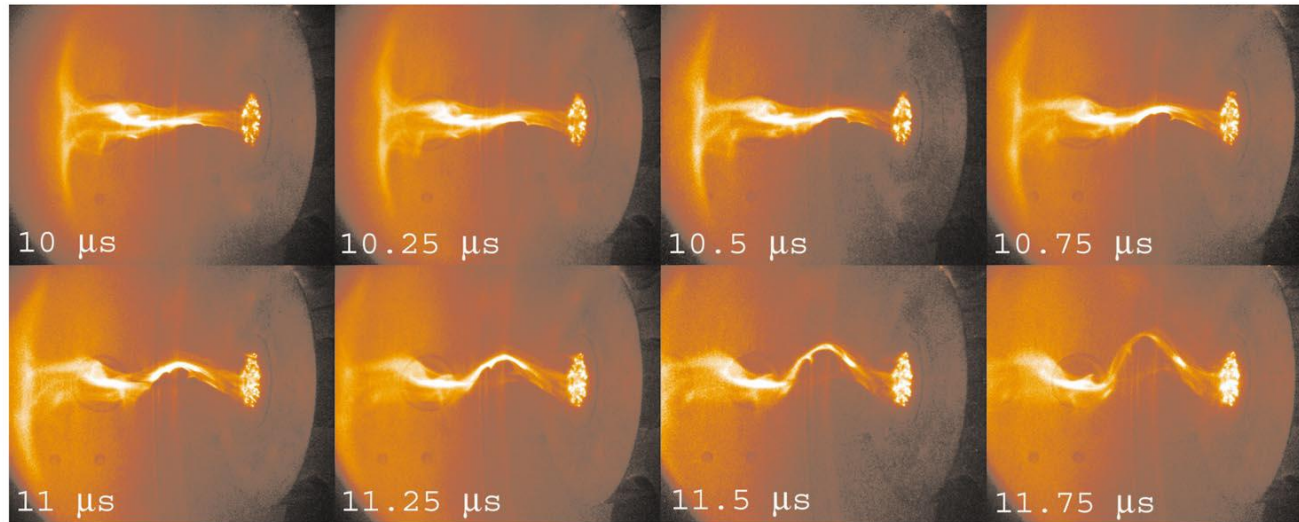
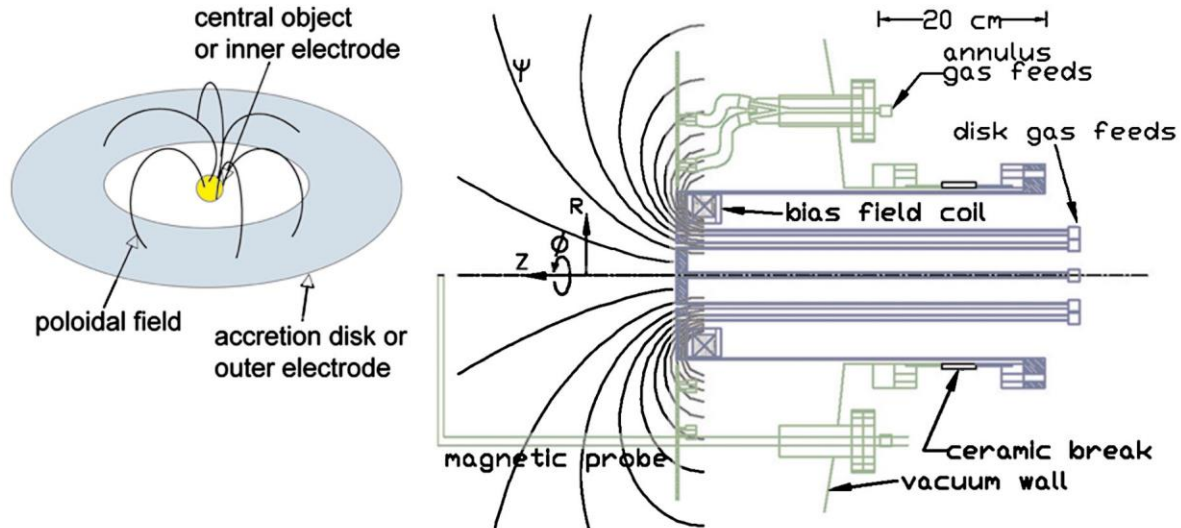
54 ns 70 ns



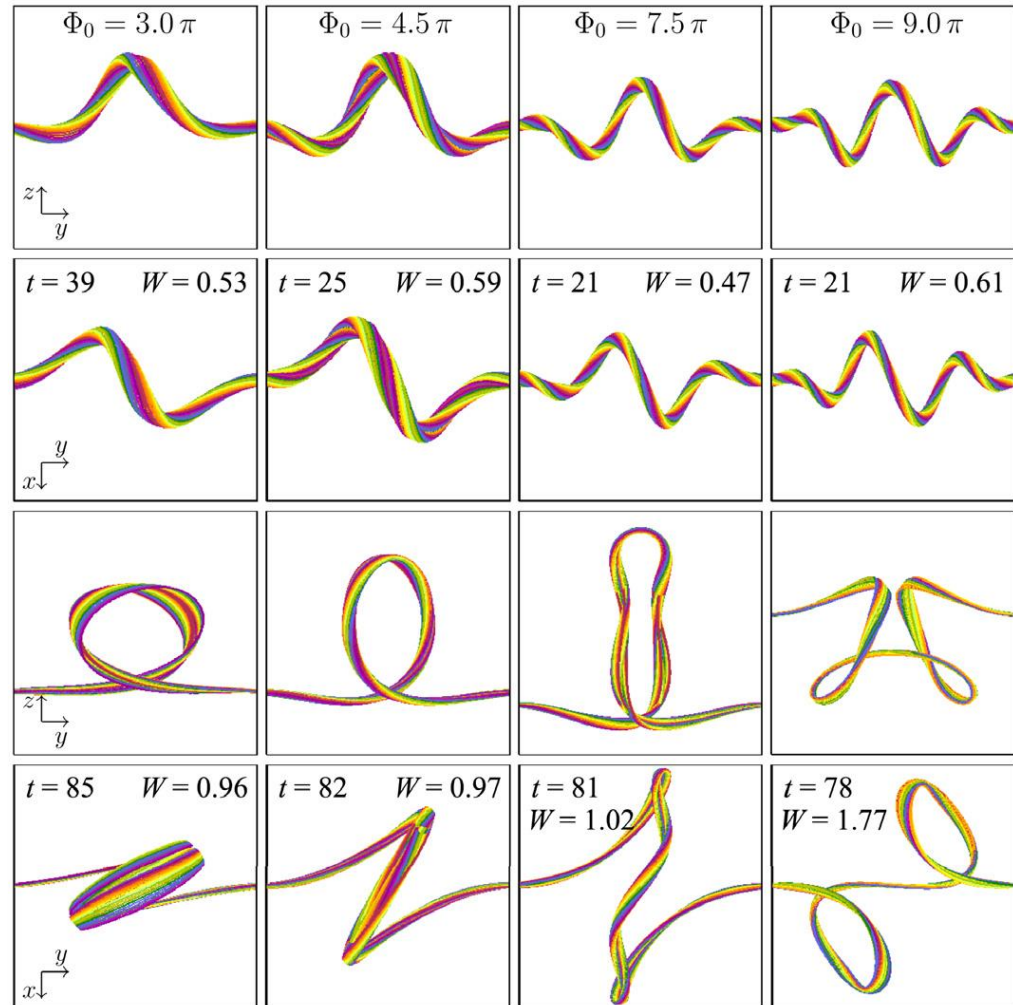
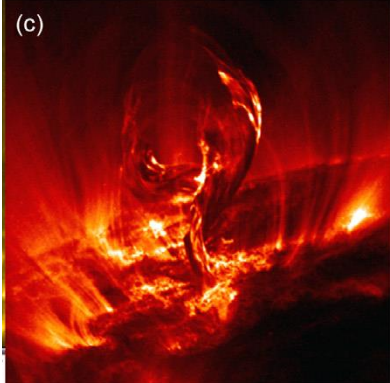
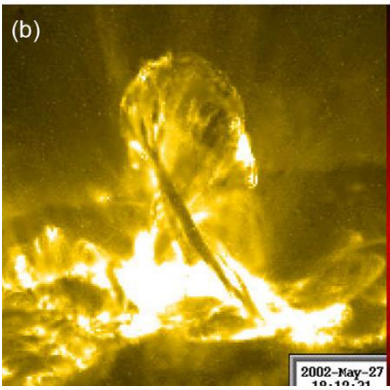
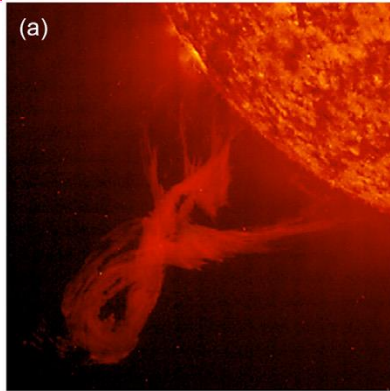
8.3 mm



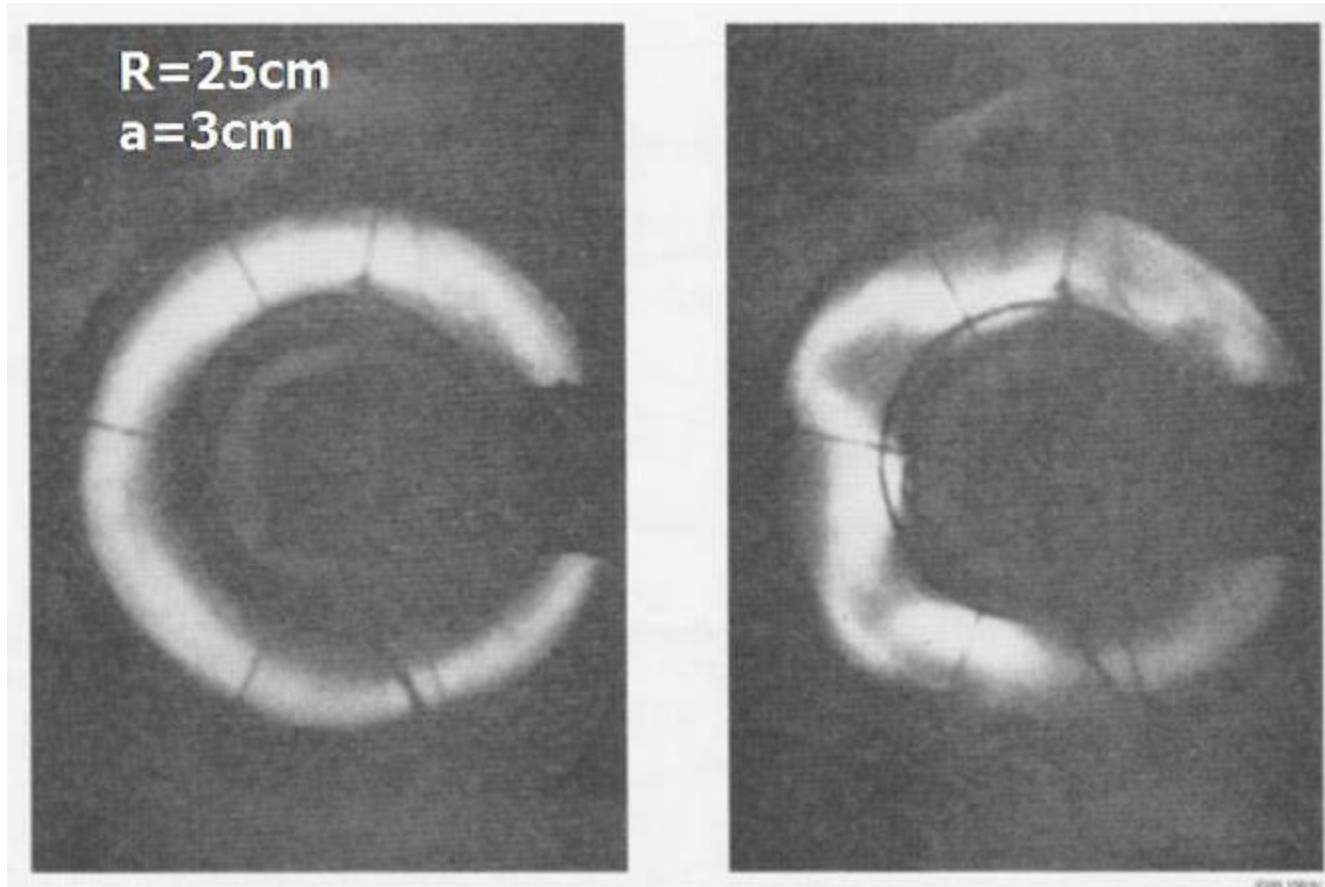
Kink instabilities in the lab



Kink instabilities in space



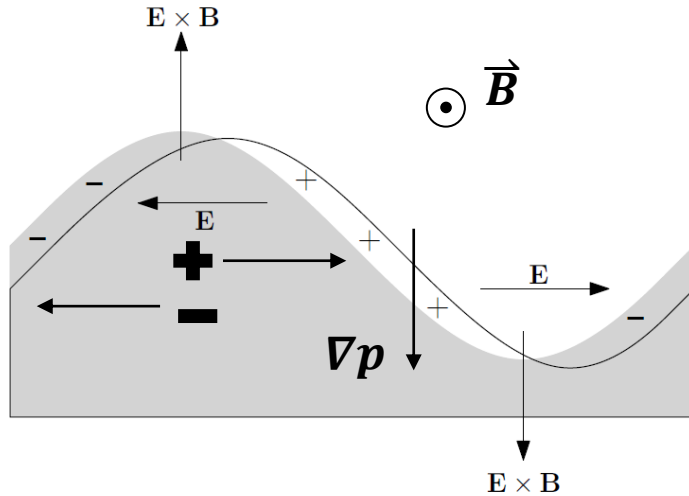
Kink instability in Tokamak



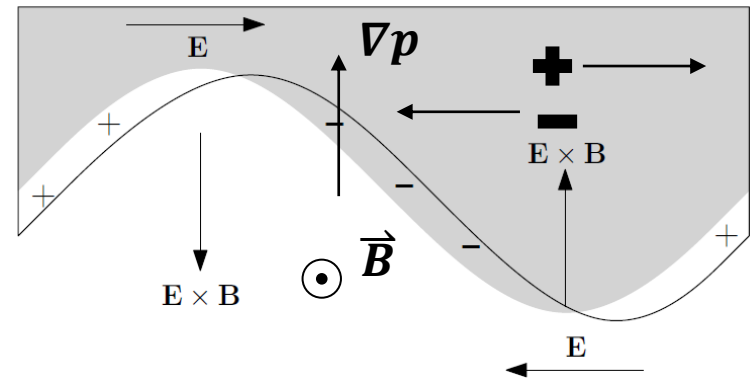
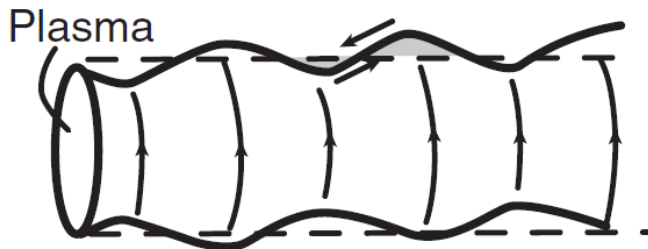
Pressure driven instability – interchange perturbations



- Unstable: bad curvature $\vec{R}_c \cdot \nabla p < 0$
- stable: good curvature $\vec{R}_c \cdot \nabla p > 0$

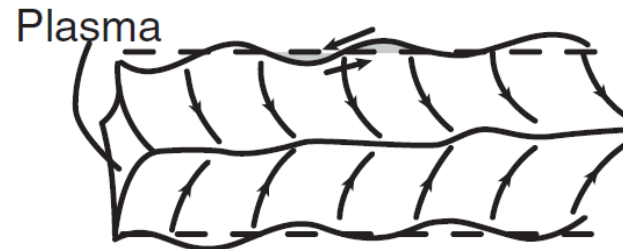


Unstable plasma-vacuum interface



\vec{R}_c Curvature
 $\vec{R}_c \times \vec{B}$ Curvature drift
 \vec{B}

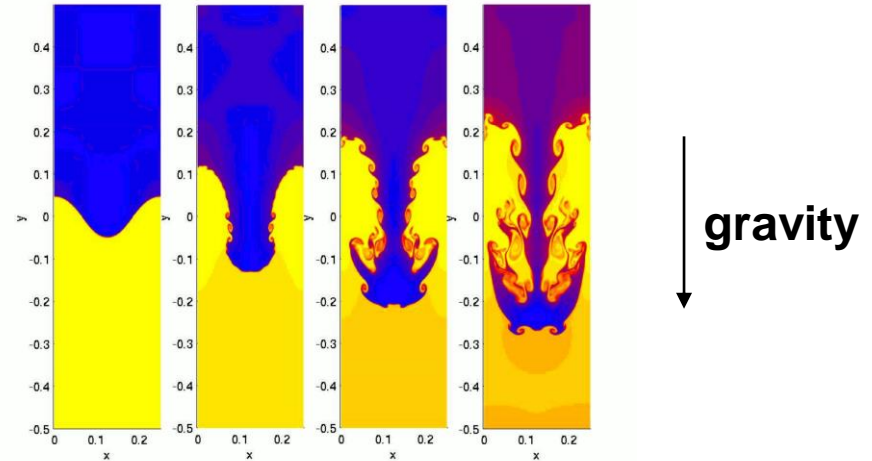
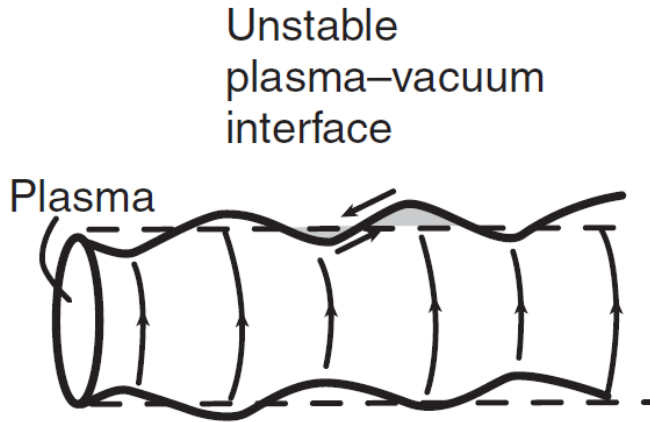
Stable plasma-vacuum interface



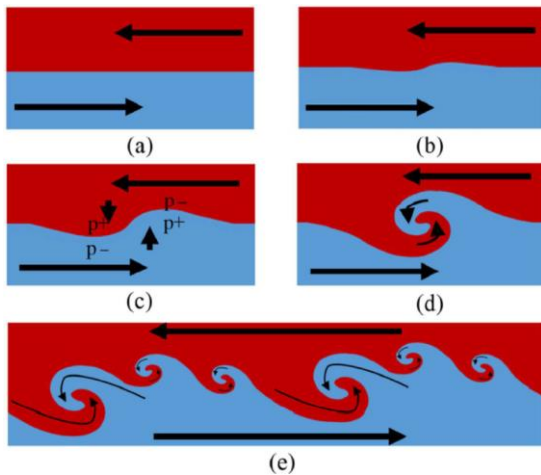
Rayleigh-Taylor instability



- Rayleigh-Taylor instability

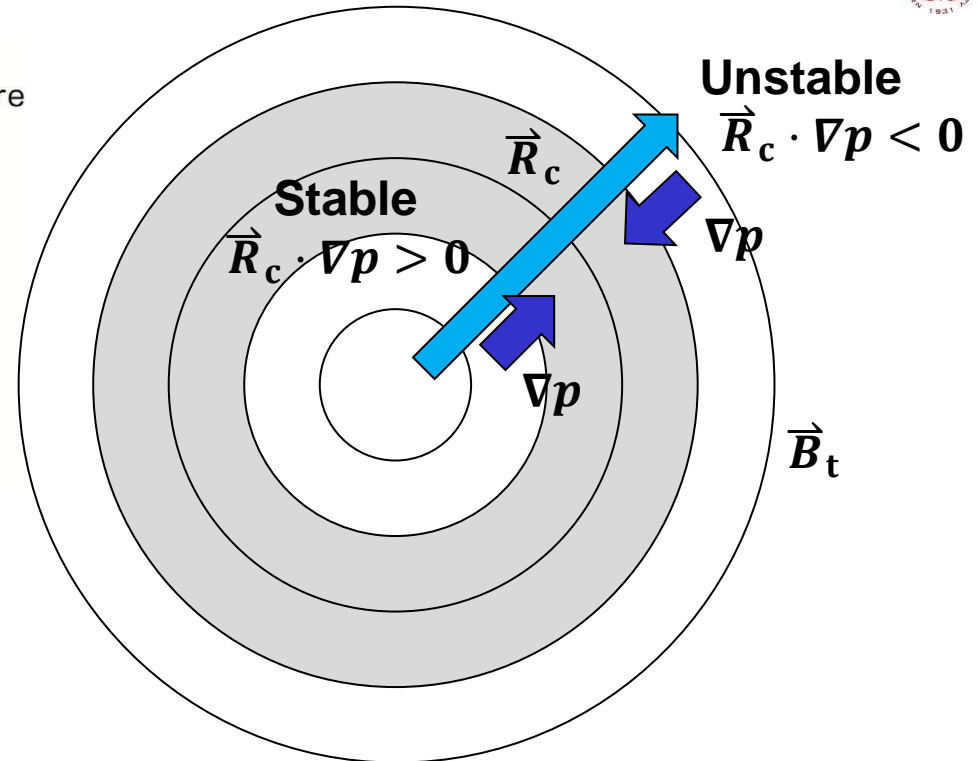
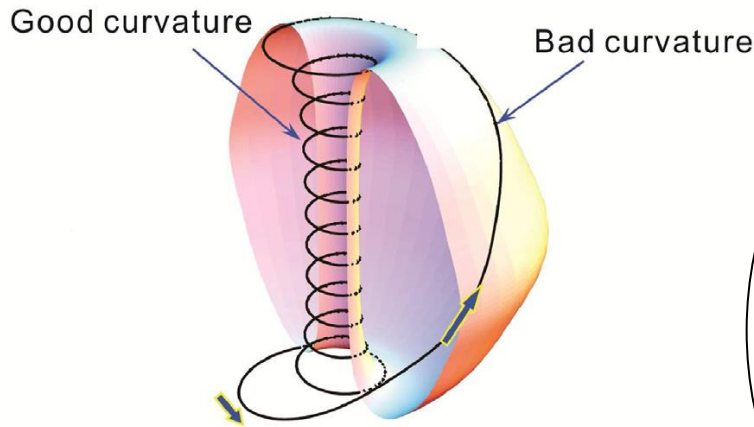


- Kelvin-Helmholtz instability



https://en.wikipedia.org/wiki/Rayleigh%E2%80%93Taylor_instability
https://en.wikipedia.org/wiki/Kelvin%E2%80%93Helmholtz_instability
 Xie Lei et al, Energy Report 7, 2262 (2021)

Pressure driven instability – interchange perturbations



- Suydam criterion for cylindrical plasmas:

$$\mu_0 \frac{2r^2}{B_\theta^2} \frac{1}{s^2} \vec{R}_c \cdot \nabla p > -\frac{1}{4} \quad \text{Shear: } s = \frac{r}{q} \frac{dq}{dr}$$

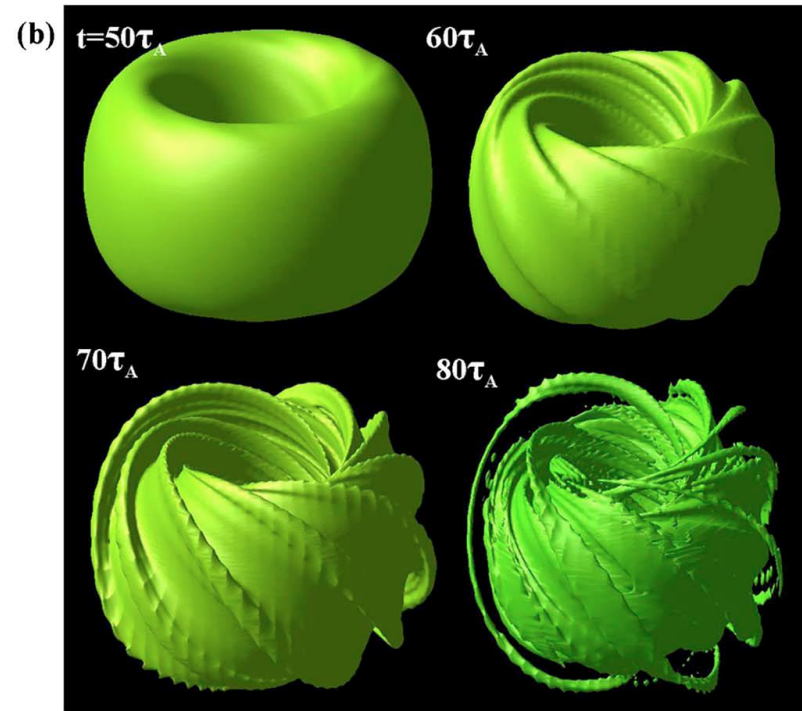
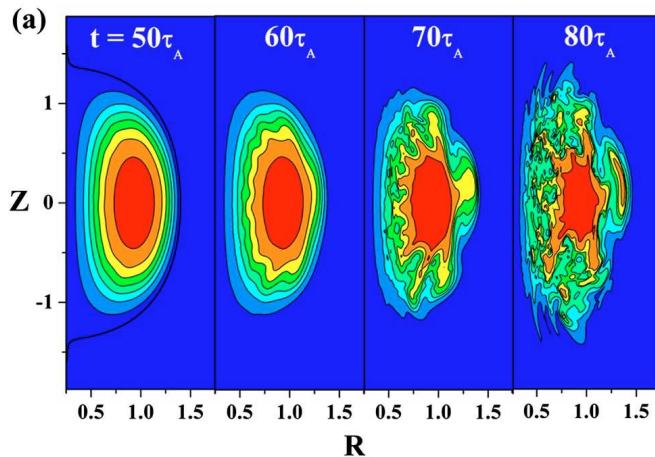
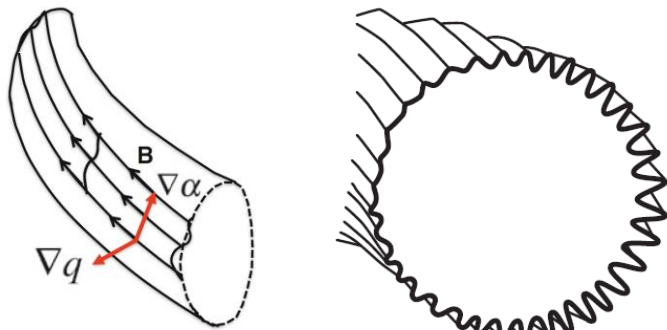
- Mercier criterion for tokamak:

$$D = -\mu_0 \frac{2r}{B^2} \frac{1}{s^2} \frac{dp}{dr} (1 - q^2) < \frac{1}{4}$$

Ballooning mode – show wavelength mode



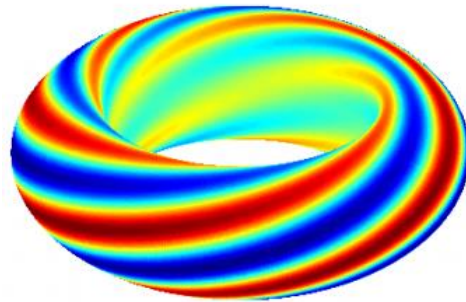
$$\delta W_F = \frac{1}{2} \int d\vec{r} \left[\frac{|\vec{Q}_\perp|^2}{\mu_o} + \frac{B^2}{\mu_o} |\nabla \cdot \vec{\xi}_\perp + 2 \vec{\xi}_\perp \cdot \vec{\kappa}|^2 + \gamma p |\nabla \cdot \vec{\xi}|^2 - 2(\vec{\xi}_\perp \cdot \nabla p)(\vec{\kappa} \cdot \vec{\xi}_\perp^*) - J_\parallel (\vec{\xi}_\perp^* \times \vec{b}) \cdot \vec{Q}_\perp \right]$$



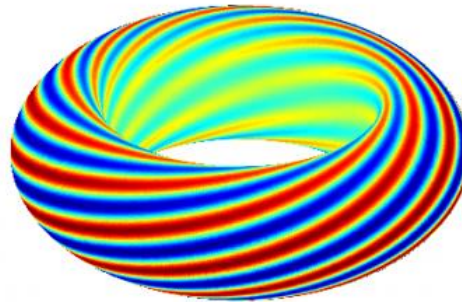
Ballooning mode – show wavelength mode



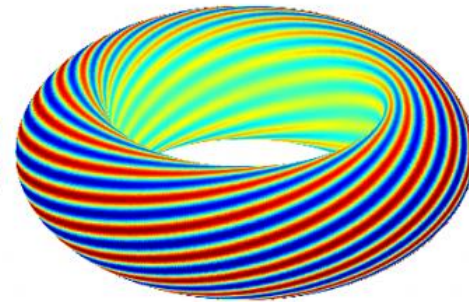
Tokamak Ballooning Mode Visualization (Artificial)
($m=5, n=4$) ($m=10, n=8$) ($m=15, n=12$)



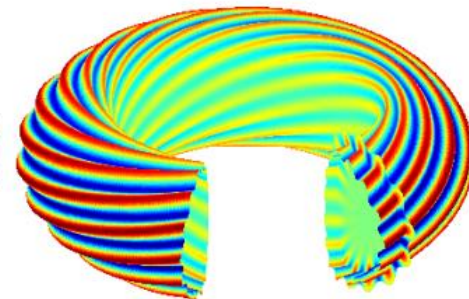
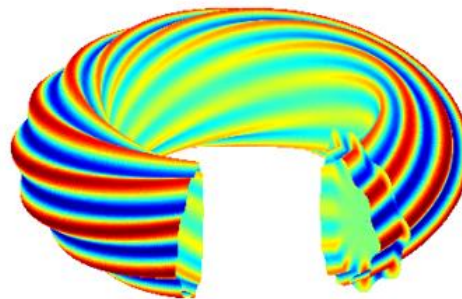
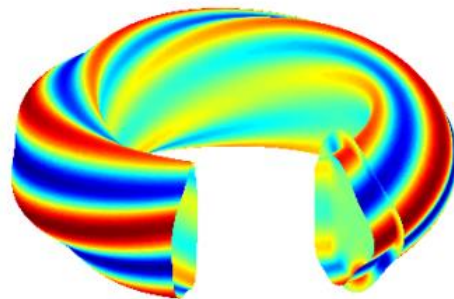
($m=5, n=4$)



($m=10, n=8$)



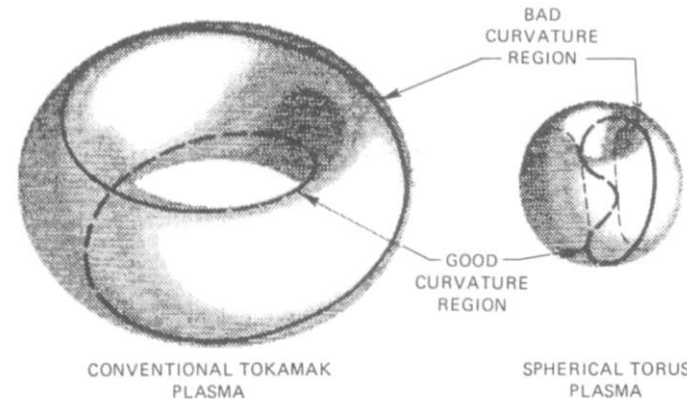
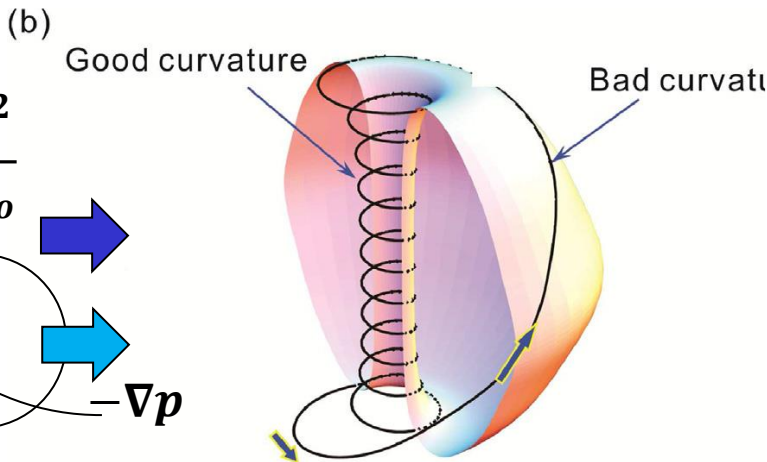
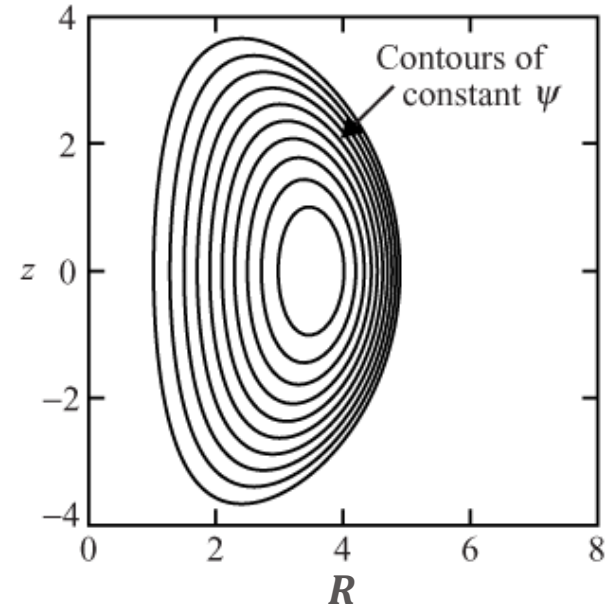
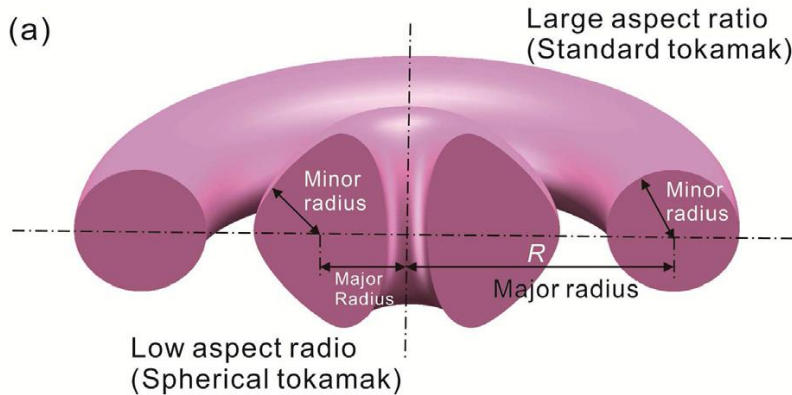
($m=15, n=12$)



The Spherical tokamak



- Aspect ratio $R_0/a \sim 1.6$

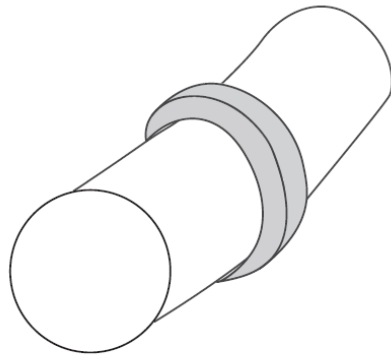


The Spherical tokamak

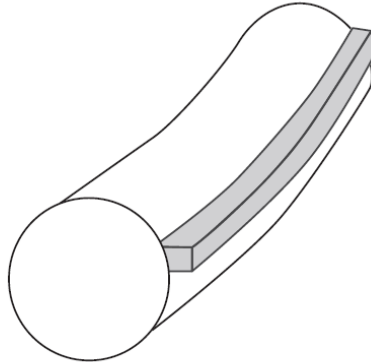


- **Aspect ratio $R_0/a \sim 1.6$**
- **Advantages:**
 - **Higher β_t limit.**
 - **A compact design almost spherical in appearance.**
- **Challenges:**
 - **Minimum space is given in the center of the torus to accommodate the toroidal field coils.**
 - **With a very compact design the technology associated with the construction and maintenance of the device may be more difficult than for a “normal” tokamak.**
 - **Large currents will have to be driven noninductively, a costly and physically difficult requirement.**

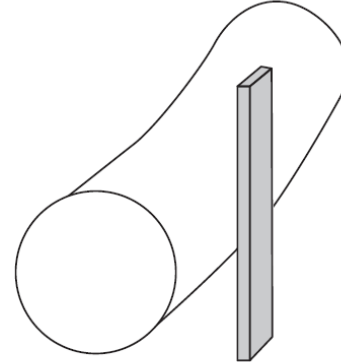
Limiter protects the vacuum chamber from plasma bombardment and defines the edge of the plasma



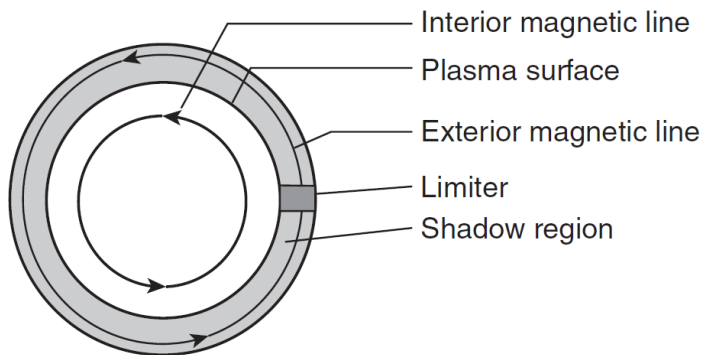
Poloidal limiter



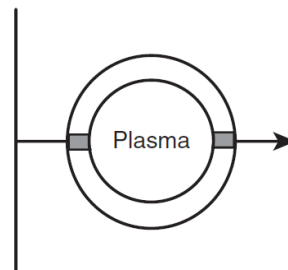
Toroidal limiter



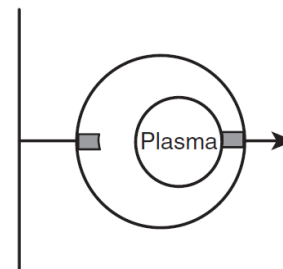
Rail limiter



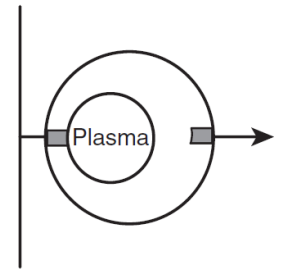
- **Vertical field is correct.**



- **Vertical field is too small.**



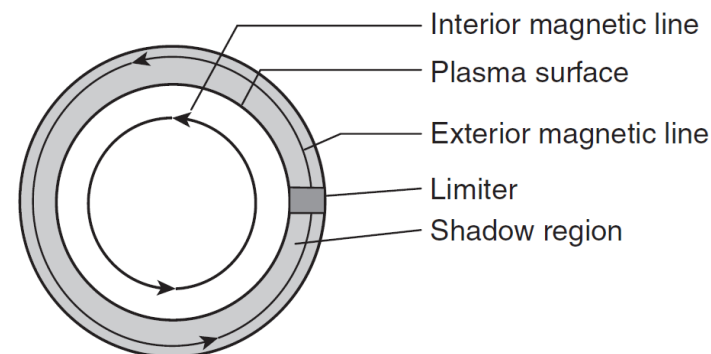
- **Vertical field is too large.**



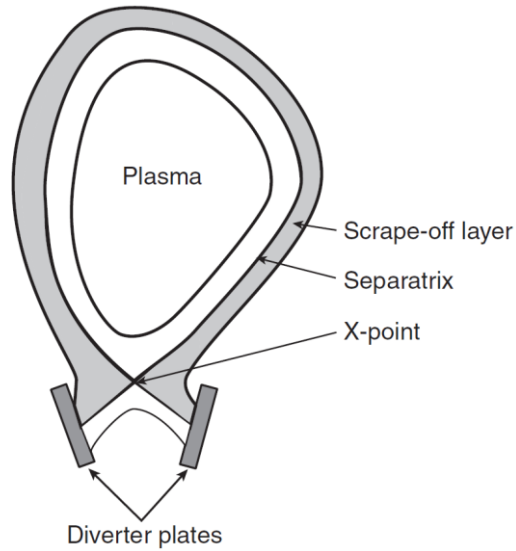
Limiter protects the vacuum chamber from plasma bombardment and defines the edge of the plasma



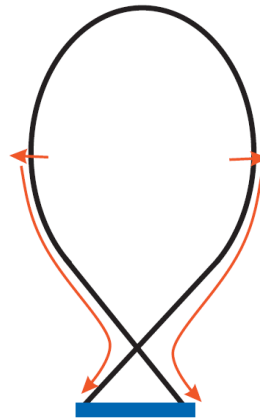
- A mechanical limiter is a robust piece of material, often made of tungsten, molybdenum, or graphite placed inside the vacuum chamber.
- Some of the particles of the limiter surface may escape. Neutral particles can penetrate some distance into the plasma before being ionized.
- The high-z impurities can lead to significant additional energy loss in the plasma through radiation.
- In ignition experiments and fusion reactors, the bombardment is more intense and extends over longer periods of time. In addition, if the impurity level is too high, it may not be possible to achieve a high enough temperature to ignite.



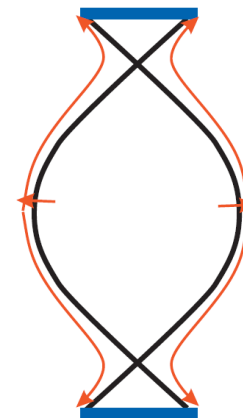
The magnetic divertor – guide a narrower layer of magnetic lines away from the edge of the plasma



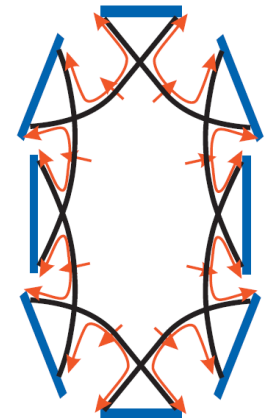
- **Single-null poloidal-field divertors for tokamak**



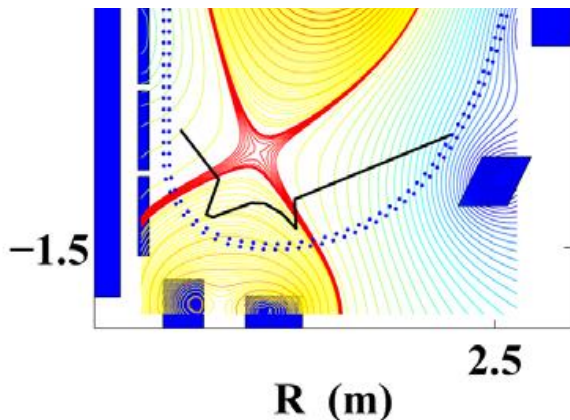
- **Double-null poloidal-field divertors for tokamak**



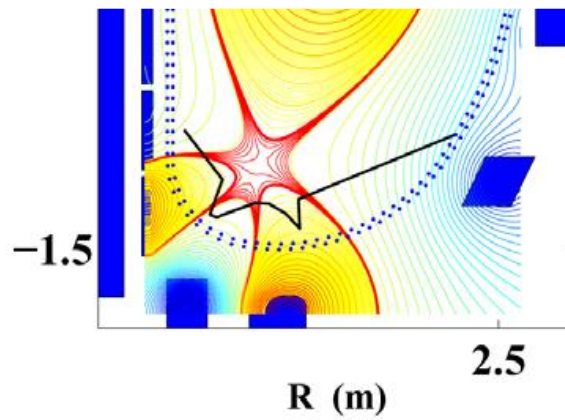
- **Island divertor for stellarators**



- **Standard**



- **Snowflake**



Y. Feng, Nucl. Fusion, **46**, 807 (2006)
 L Xue *et al*, Plasma Phys. Control. Fusion **58**, 055005 (2016)

Pros and cons of a divertor



- **Advantages:**
 - The collector plate is remote from the plasma. There is space available to spread out the magnetic lines.
 - A lower intensity of particles and energy bombard the collector plate leading to a longer replacement time.
 - It is more difficult for impurities to migrate into the plasma.
 - There are longer distance distances to travel and if a neutral particle becomes ionized before or during the time it crosses the divertor layer on its way toward the plasma, its parallel motion then carries it back to the collector plate.
 - The larger divertor chamber provides more access to pump out impurities.
 - The plasma edge is not in direct contact with a solid material such as a limiter.
- **Disadvantages:** larger and more complex system and more expensive.

Course Outline

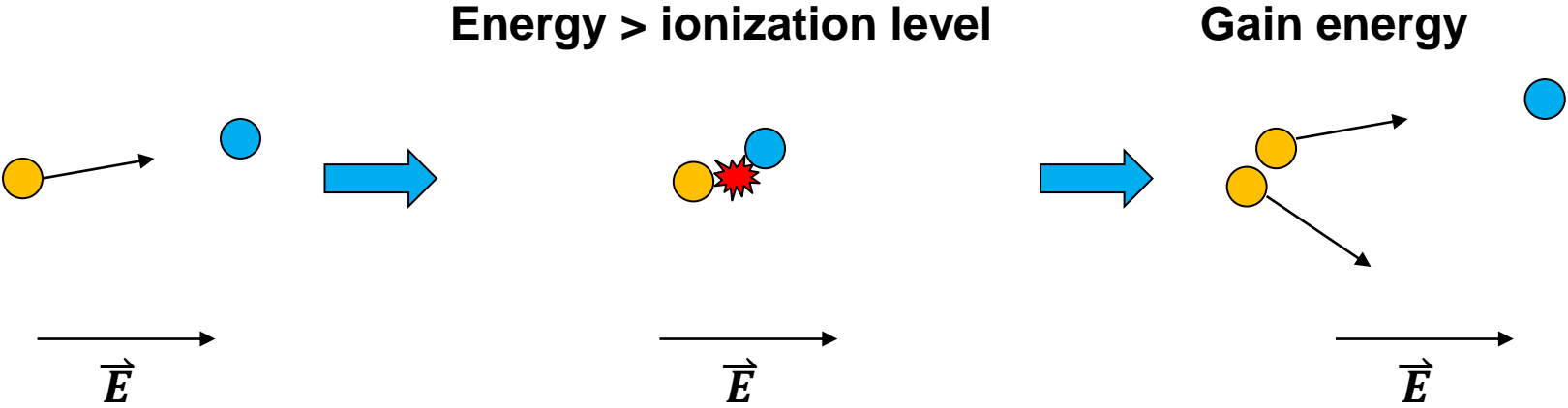


- **Magnetic confinement fusion (MCF)**
 - Gyro motion, MHD
 - 1D equilibrium (z pinch, theta pinch)
 - Drift: ExB drift, grad B drift, and curvature B drift
 - Tokamak, Stellarator (toroidal field, poloidal field)
 - Magnetic flux surface
 - 2D axisymmetric equilibrium of a torus plasma: Grad-Shafranov equation.
 - Stability (Kink instability, sausage instability, Safety factor Q)
 - Central-solenoid (CS) start-up (discharge) and current drive
 - CS-free current drive: electron cyclotron current drive, bootstrap current.
 - Auxiliary Heating: ECRH, Ohmic heating, Neutral beam injection.

Collisions play an important role in ionization process



- At the microscopic level, breakdown requires the presence of sufficiently energy charge particles that have acquired enough energy from the applied electric field between two energy-dissipating collisions to ionize the material and to create more charge particles.



In most cases, electrons dominate the breakdown process since its mobility is much larger than that of ions



$$E_k = \frac{1}{2}mv^2 \quad v = \sqrt{\frac{2E_k}{m}} \quad E_k \sim kT$$

Collision time: $t = \frac{s}{\sqrt{\frac{2E_k}{m}}} \sim \frac{n^{-1/3}}{\sqrt{T}} \sqrt{m}$ $n = \frac{\#}{V} \sim \frac{\#//}{S^3}$ $s \sim n^{-1/3}$

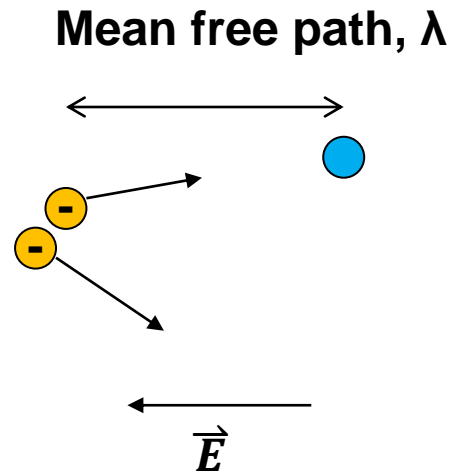
$$\frac{m_i}{m_e} \sim 2000 \times \text{Atomic mass}$$

$$\frac{t_i}{t_e} \sim 45 \times \sqrt{A}$$

Mean free path is important in ionization process



- For an electron to acquire enough energy between collisions, its mean free path in the material must be sufficiently long.



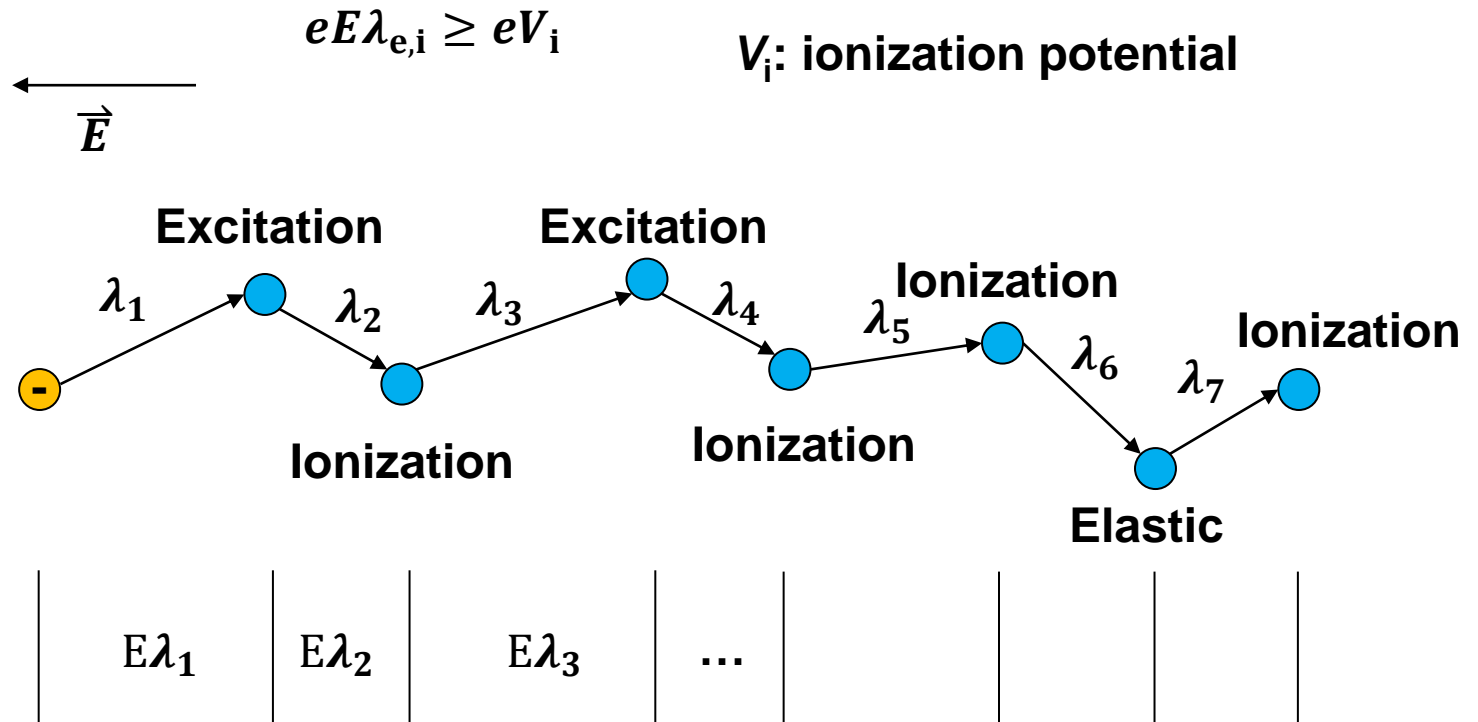
$$E_k = e \times E \times \lambda = eV$$

Electron impact ionization is the most important process in a breakdown of gases

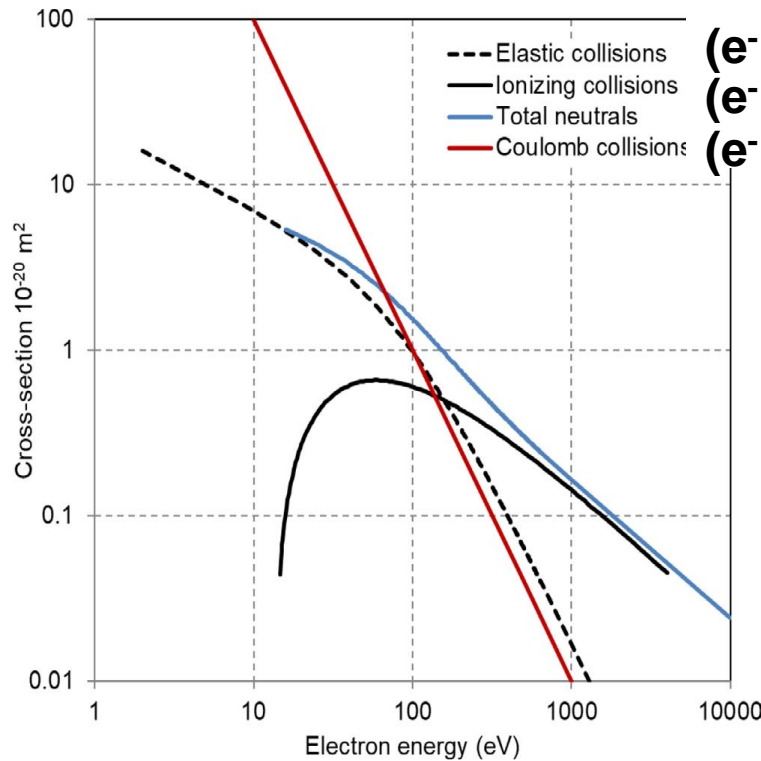


- Electron impact ionization: $A + e^- \rightarrow A^+ + e^- + e^-$

- The most important process in the breakdown of gases but is not sufficient alone to result in the breakdown.



Collision cross-sections of elastic, ionizing collisions between e⁻ and H₂ and coulomb collisions



--- Elastic collisions (e⁻ vs H₂)
 — Ionizing collisions (e⁻ + H₂ → 2e⁻ + H⁺ + H)
 — Total neutrals
 — Coulomb collisions (e⁻ vs H⁺)

$$\sigma_{\text{elastic}, m^2} = \frac{1.75 \times 10^{-16}}{(W_{e,eV}^{1.5} + 750)\sqrt{W_{e,eV}}}$$

$$\sigma_{\text{ionizing}, m^2} \sim 3 \times 10^{-20} \left(\ln \epsilon - 0.69 + \frac{0.66}{\epsilon} \right) \epsilon^{-1}$$

$$\epsilon = \frac{W_e}{E_{\text{ion}}} \quad E_{\text{ion}} \sim 15 \text{ eV for H}_2$$

$$\sigma_{\text{coulomb}} = \frac{e^4}{4\pi\epsilon_0^2 m_e^2 v_e^2} \ln \Lambda$$

$$= \frac{e^4}{16\pi\epsilon_0^2 W_e^2} \ln \Lambda \sim 10^{-16} W_e^{-2}$$

for $\ln \Lambda \sim 13 - 15$

$$\nu = n v_E \sigma$$

$$\lambda = \frac{1}{n \sigma}$$

Townsend avalanche process for Tokamak breakdown



- The first Townsend coefficient α : the number of ionizing collisions made on the average by an electron as it travels 1 m along the electric field:

$$\alpha \sim \frac{1}{\lambda_i} = \frac{\nu_{ei}}{\bar{v}_e} = \frac{n_0 \langle \sigma v_e \rangle_{ne}}{\bar{v}_e} = \frac{p}{T} \frac{\langle \sigma v \rangle_{ne}}{\bar{v}_e} \equiv Ap \qquad A \equiv \frac{1}{T} \frac{\langle \sigma v \rangle_{ne}}{\bar{v}_e}$$

- Number of primary electrons with energy higher than the ionization potential:

$$dn_e = -n_e \frac{dx_i}{\lambda_i} \Rightarrow \frac{n_e(x_i)}{n_{e0}} = \exp\left(-\frac{x_i}{\lambda_i}\right)$$

$$\alpha \equiv \frac{\text{\# / ionization collisions}}{\text{per electron}} \times (\text{\# / electron with } E > \text{ ionization potential})$$

$$= \frac{1}{\lambda_i} \frac{n_e(x_i)}{n_{e0}} = \frac{1}{\lambda_i} \exp\left(-\frac{x_i}{\lambda_i}\right)$$

$$A = 3.83 \text{ m}^{-1}\text{Pa}^{-1} = 1060 \text{ m}^{-1}\text{Torr}^{-1}$$

$$B = 96.6 \text{ Vm}^{-1}\text{Pa}^{-1} = 35000 \text{ m}^{-1}\text{Torr}^{-1}$$

$$\alpha = Ap \exp(-Ap x_i)$$

$$\alpha = Ap \exp\left(-\frac{AV^*}{E/p}\right) \equiv Ap \exp\left(-\frac{B}{E/p}\right) \quad x_i \approx \frac{V^*}{E} \text{ where } V^* > V_i$$

- The parameters A and B must be experimentally determined.

Paschen's curve for minimum breakdown voltage



$$\alpha \sim \frac{1}{\lambda_i} = Ap \quad \alpha = Ap \exp\left(-\frac{B}{E/p}\right)$$

$$A = 3.83 \text{ m}^{-1}\text{Pa}^{-1} = 1060 \text{ m}^{-1}\text{Torr}^{-1}$$

$$B = 96.6 \text{ Vm}^{-1}\text{Pa}^{-1} = 35000 \text{ m}^{-1}\text{Torr}^{-1}$$

- For $p=1 \text{ mPa}$, $\lambda_i \sim 262 \text{ m}$, for ITER, $2\pi r_0 \sim 38 \text{ m}$ $\frac{\lambda_i}{2\pi r_0} \sim 7$

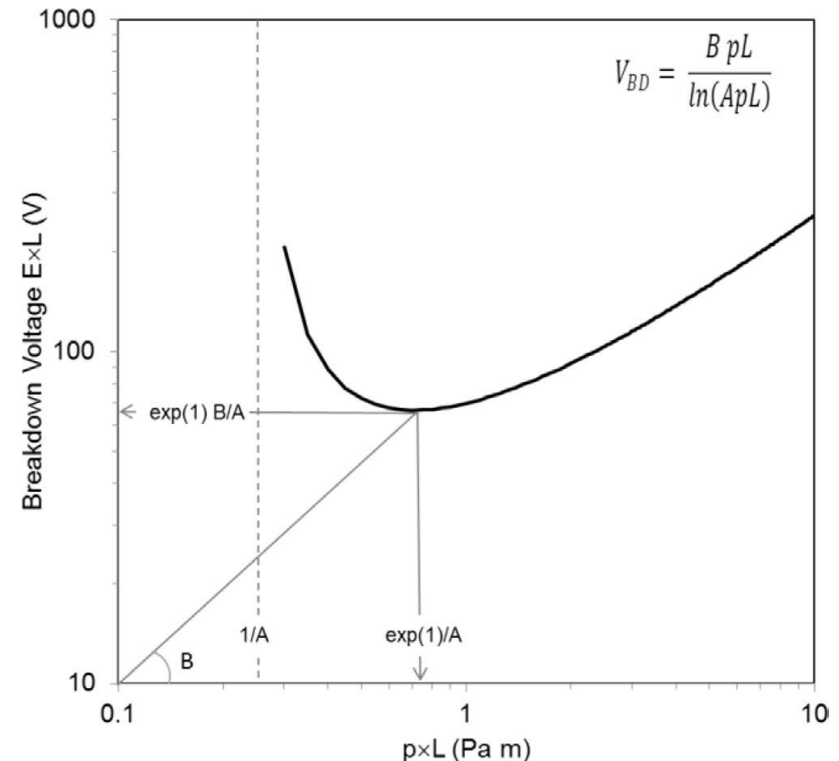
- For breakdown to happen:

$$\alpha L > 1 \quad \alpha L = ApL \exp\left(-\frac{BpL}{V_{BD}}\right) > 1$$

$$\exp\left(-\frac{BpL}{V_{BD}}\right) > \frac{1}{ApL}$$

$$-\frac{BpL}{V_{BD}} > -\ln(ApL)$$

$$V_{BD} > \frac{BpL}{\ln(ApL)} \quad E_{BD} > \frac{Bp}{\ln(ApL)}$$



Perpendicular stray-field (B_z) needs to be as small as possible



- For $p=1$ mPa, $\lambda_i \sim 262$ m, for ITER, $2\pi r_0 \sim 38$ m $\frac{\lambda_i}{2\pi r_0} \sim 7$

$$\frac{B_z}{B_T} \sim 10^{-3} \quad \lambda_i \times \frac{B_z}{B_T} = 0.26 \text{ m}$$

- For ITER,

$$E \sim E_{\text{loop}} = 0.3 \text{ V/m}$$

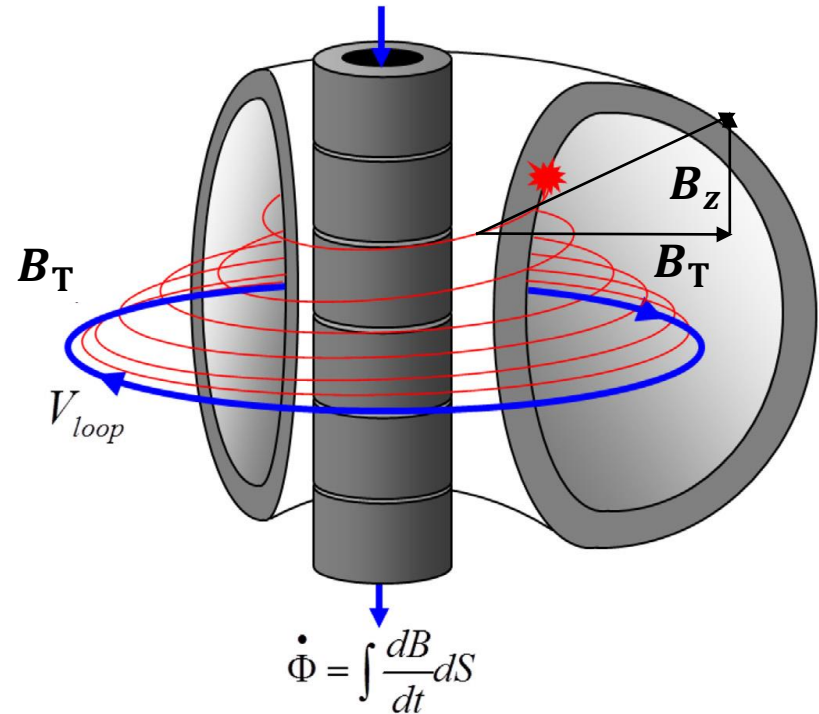
$$p = 1 \text{ mPa} \quad L_{\text{BD}} = 357 \text{ m}$$

- Required loop field:

$$E_{\text{BD}} > \frac{Bp}{\ln(ApL)}$$

$$E_{\text{BD}} > \frac{1.25 \times 10^4 P_{\text{Torr}}}{\ln(510PL_c)}$$

$$L_c = 0.25 a_{\text{eff}} \left(\frac{B_z}{B_T} \right)$$



- W/ preionization: $E_T \frac{B_z}{B_T} \geq 100 \text{ V/m}$
- Purely Ohmic discharges: $E_T \frac{B_z}{B_T} \geq 100 \text{ V/m}$

Examples or required loop electric fields

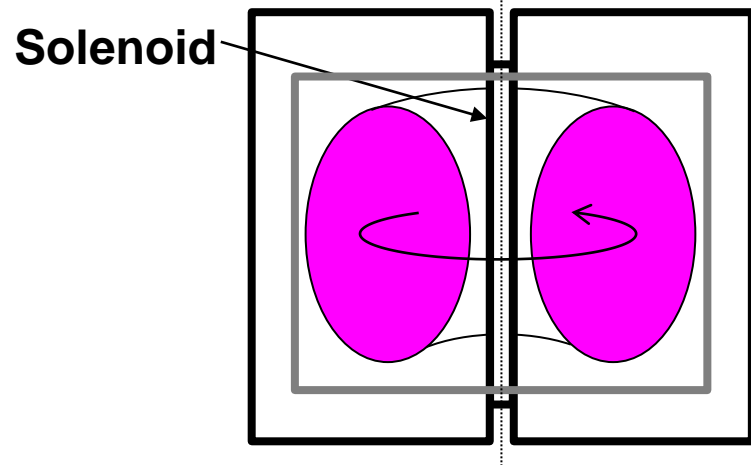
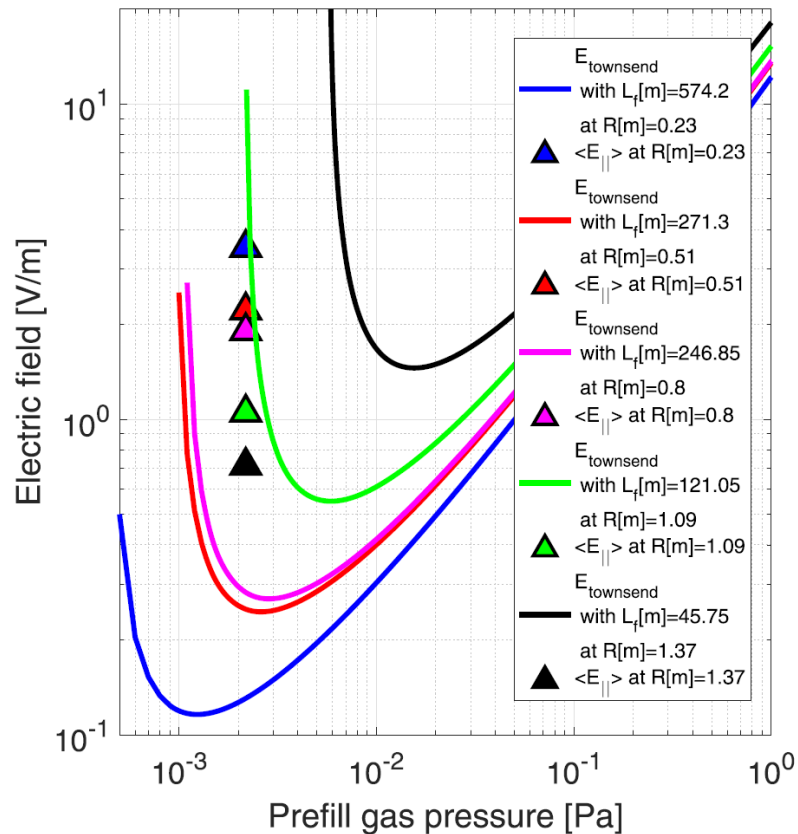


$$E_{BD} > \frac{1.25 \times 10^4 P_{Torr}}{\ln(510PL_c)}$$

$$L_c = 0.25 a_{eff} \left(\frac{B_z}{B_T} \right)$$

- W/ preionization: $E_T \frac{B_z}{B_T} \geq 100 \text{ V/m}$

- Purely Ohmic discharges: $E_T \frac{B_z}{B_T} \geq 100 \text{ V/m}$



$$V_\phi = -\frac{\partial \phi}{\partial t} \equiv M \frac{\partial I_{CS}}{\partial t}$$

$$E_\phi = -\frac{1}{2\pi r} \frac{\partial \phi}{\partial t}$$

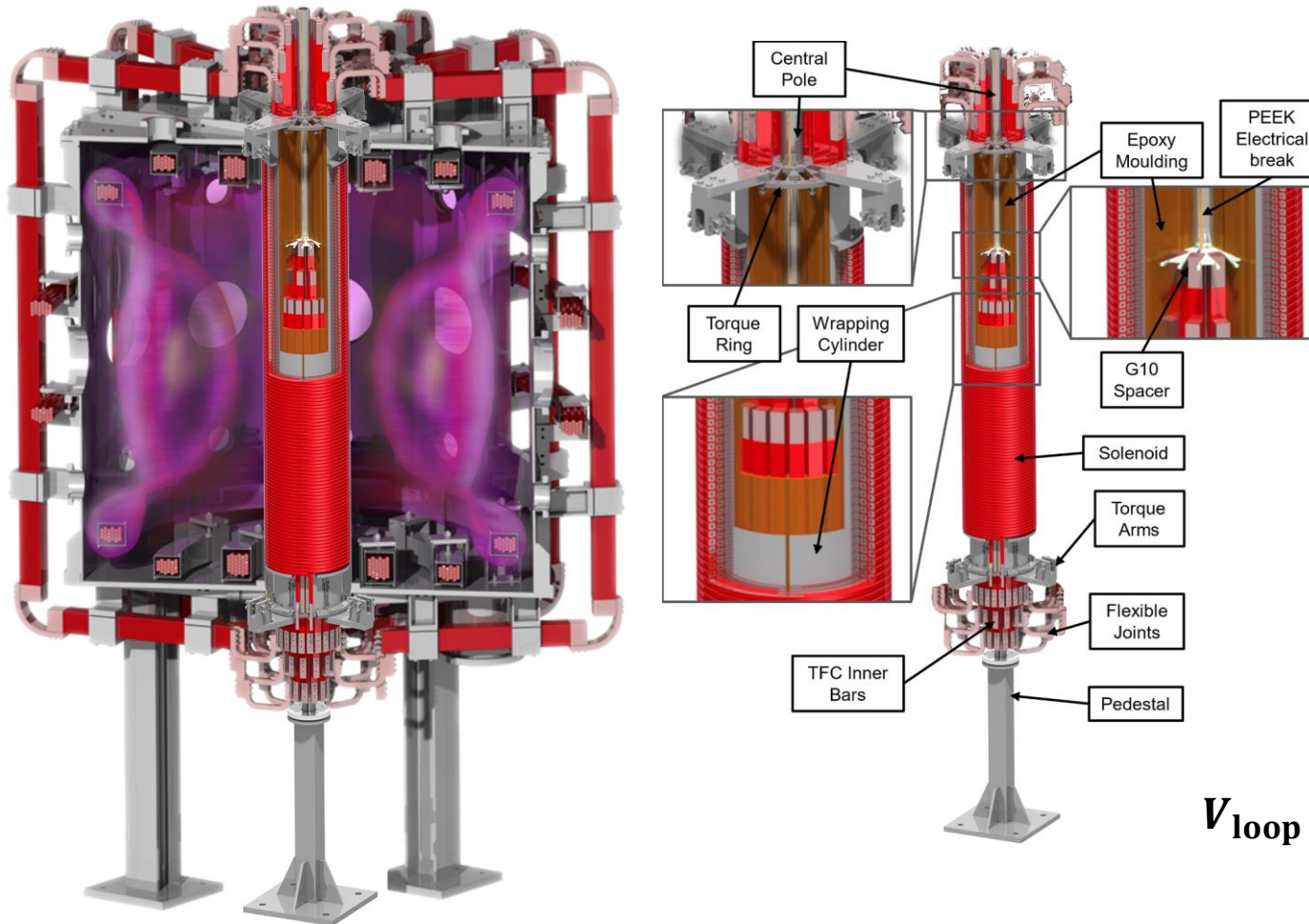
H.-T. Kim, etc., Nucl. Fusion **62**, 126012 (2022)

S. J. Doyle et al, Fusion Eng. Des. **171**, 112706 (2021)

Central solenoid can be used to provide the required loop voltage for breakdown



- SMART:



$$V_{\text{loop}} = \frac{A_{\text{sol}} \mu N_{\text{sol}}}{L_{\text{sol}}} \frac{dI_{\text{sol}}}{dt}$$

Solenoid can be used to drive the plasma current

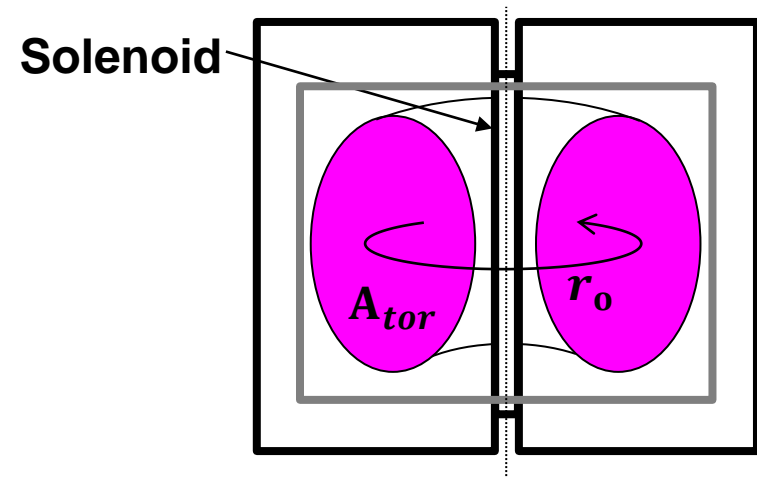


$$L_{\text{tor}} \frac{dI}{dt} + IR = V_{\text{loop}} = M \frac{dI_{\text{sol}}}{dt}$$

$$L_{\text{tor}} = \mu_0 r_0 \left(\ln \left(\frac{8r_0}{a} \right) - 1.5 \right)$$

$$R_{\text{spitzer}} = \eta_{\text{spitzer}} \frac{2\pi r_0}{A_{\text{tor}}}$$

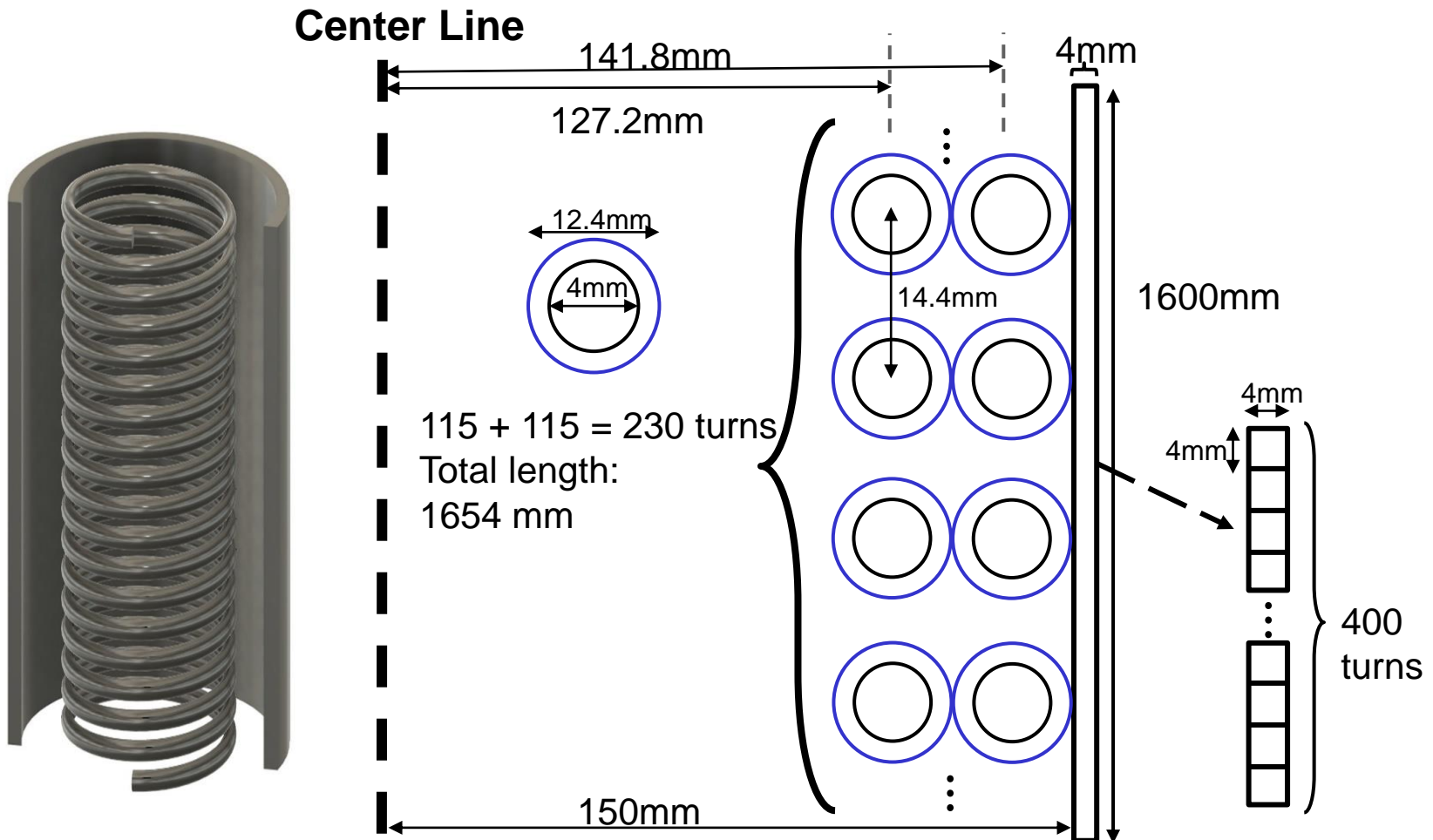
$$\eta_{\text{spitzer}} = 5.2 \times 10^{-3} Z \ln \Lambda T_{e,(\text{eV})}^{-3/2}$$



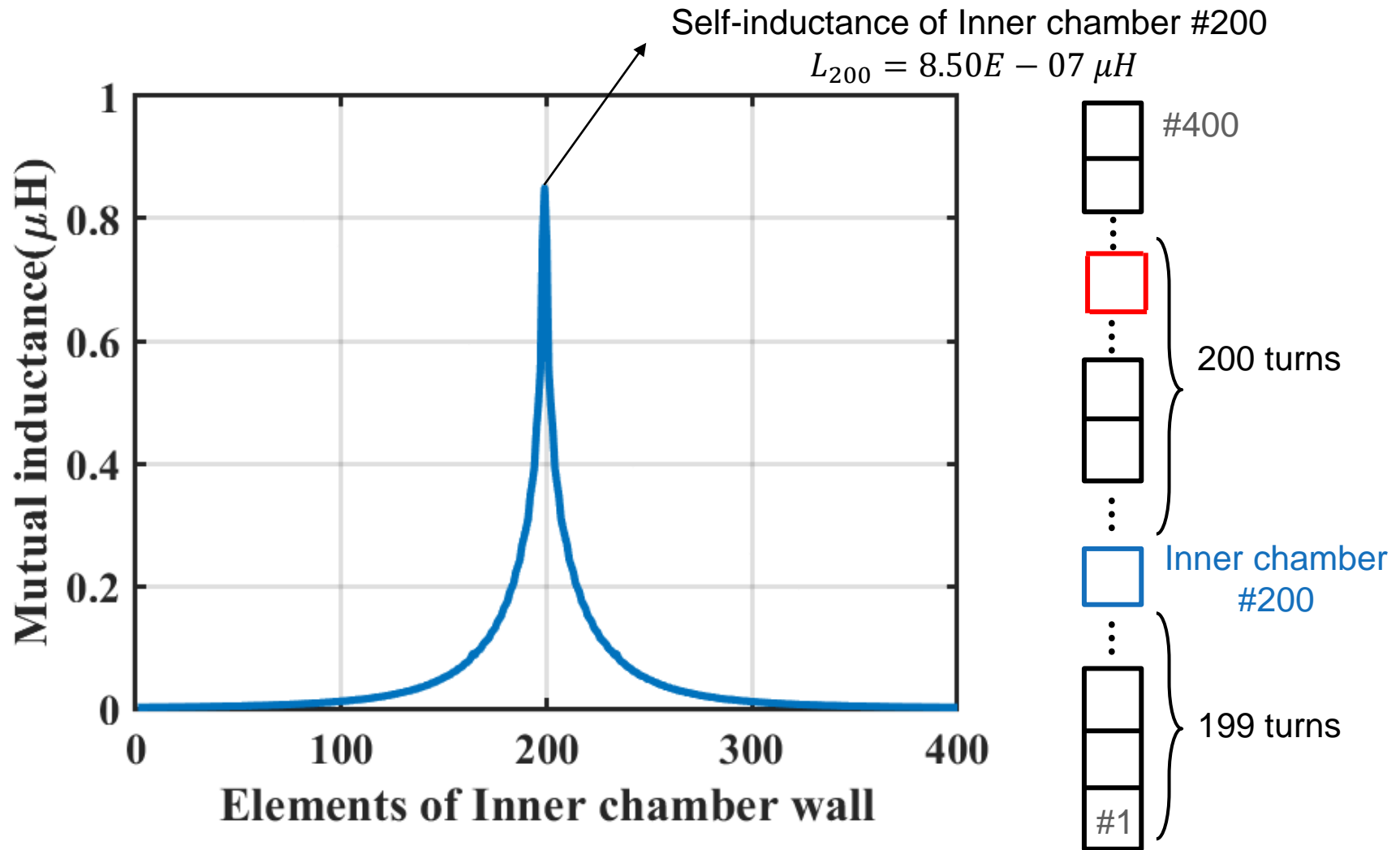
Eddy current needed to be considered



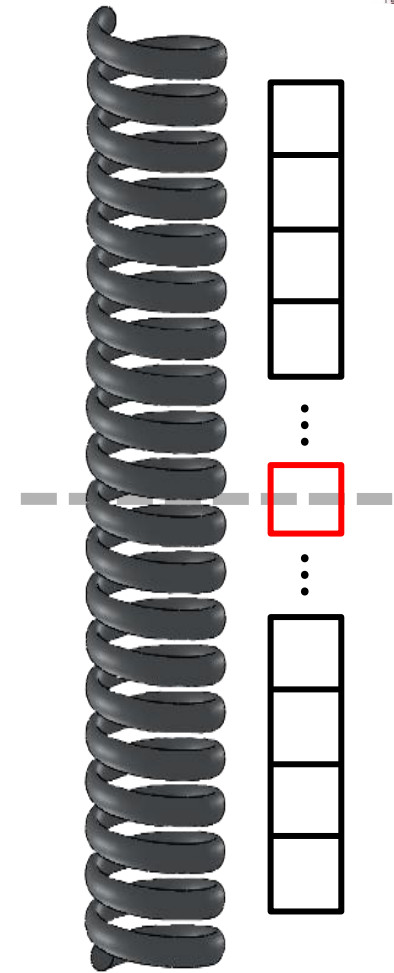
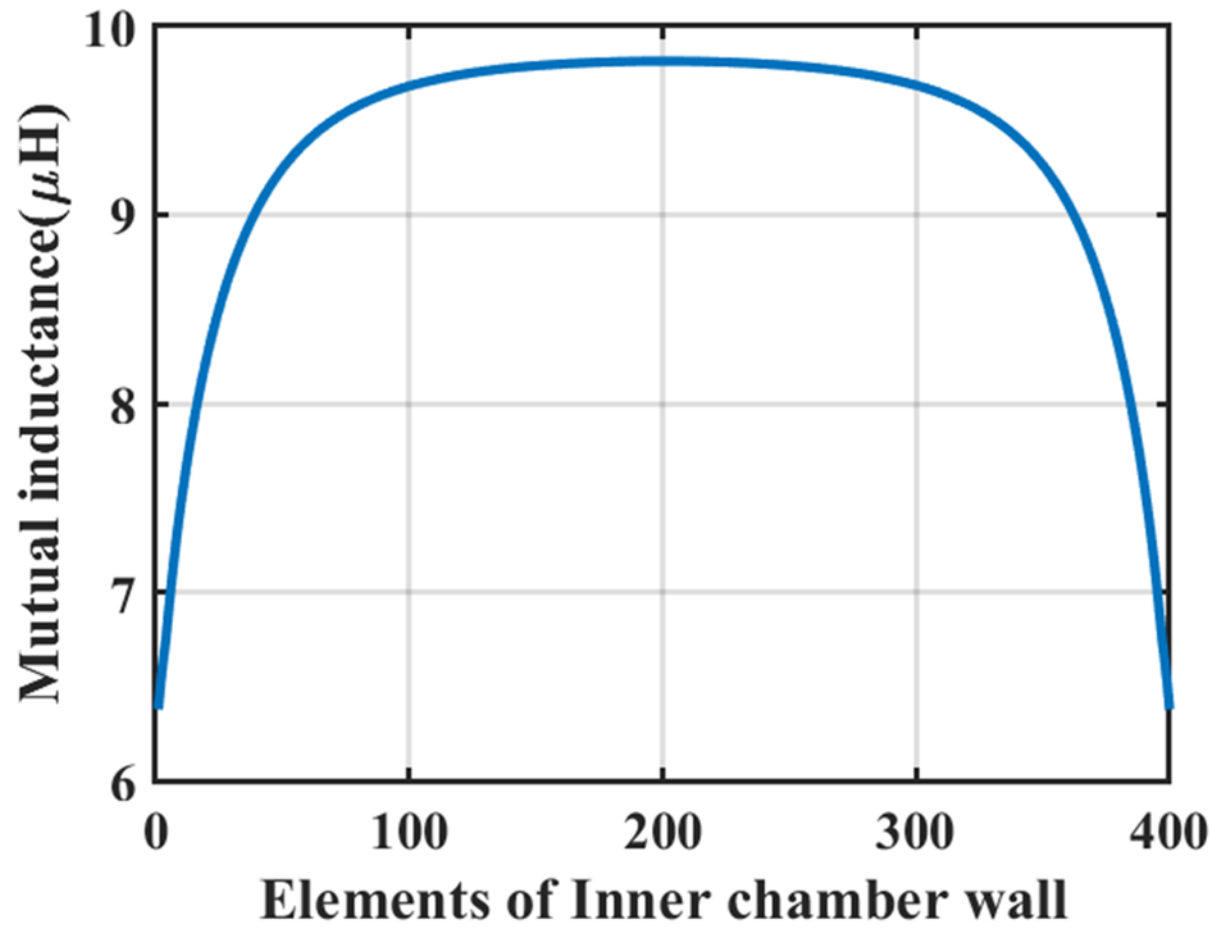
$$\overleftrightarrow{M} \frac{d\vec{I}}{dt} + \overleftrightarrow{R}_\Omega \vec{I} = \vec{V} \quad \overleftrightarrow{M} \frac{\vec{I}' - \vec{I}}{\Delta t} + \overleftrightarrow{R}_\Omega \vec{I} = \vec{V} \quad \vec{I}' = \left(\overleftrightarrow{1} - \Delta t \overleftrightarrow{M}^{-1} \overleftrightarrow{R}_\Omega \right) \vec{I} + \Delta t \overleftrightarrow{M}^{-1} \vec{V}$$



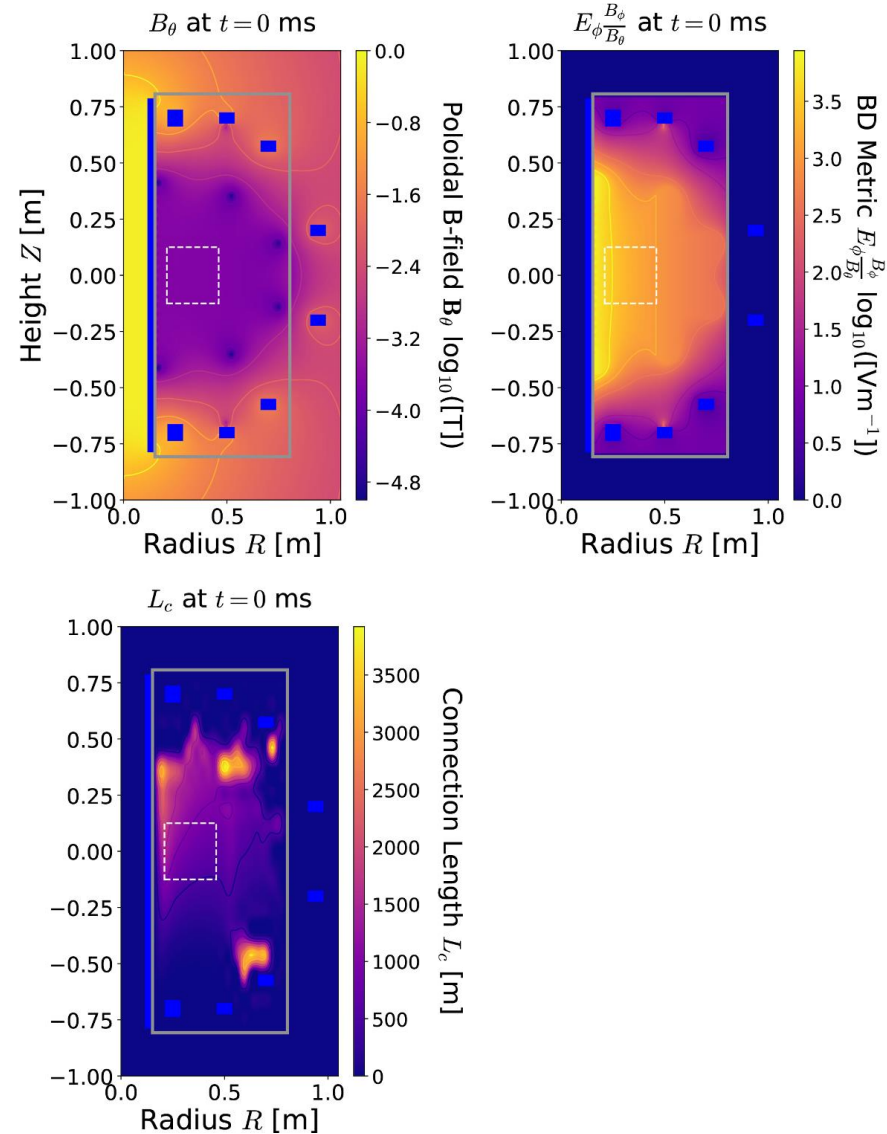
The mutual inductance between inner chamber element #200 and other elements



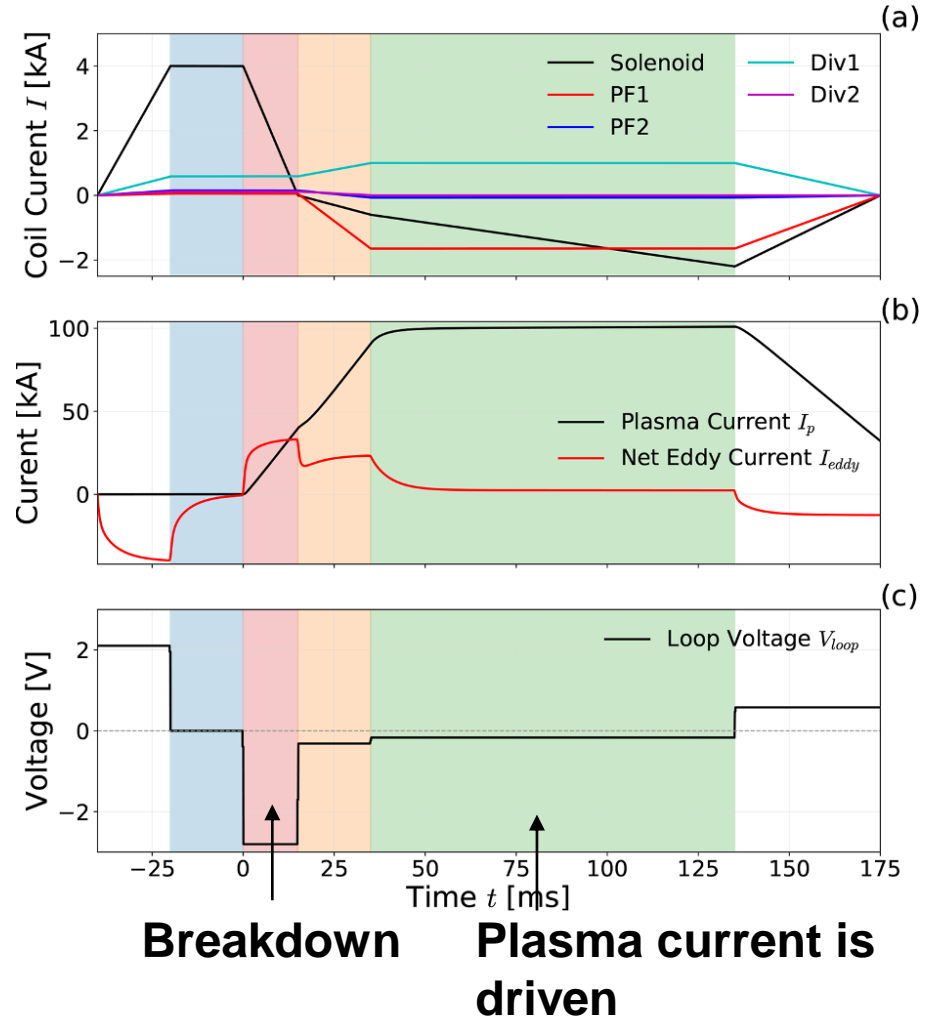
The mutual inductance between the central solenoid and other chamber wall elements



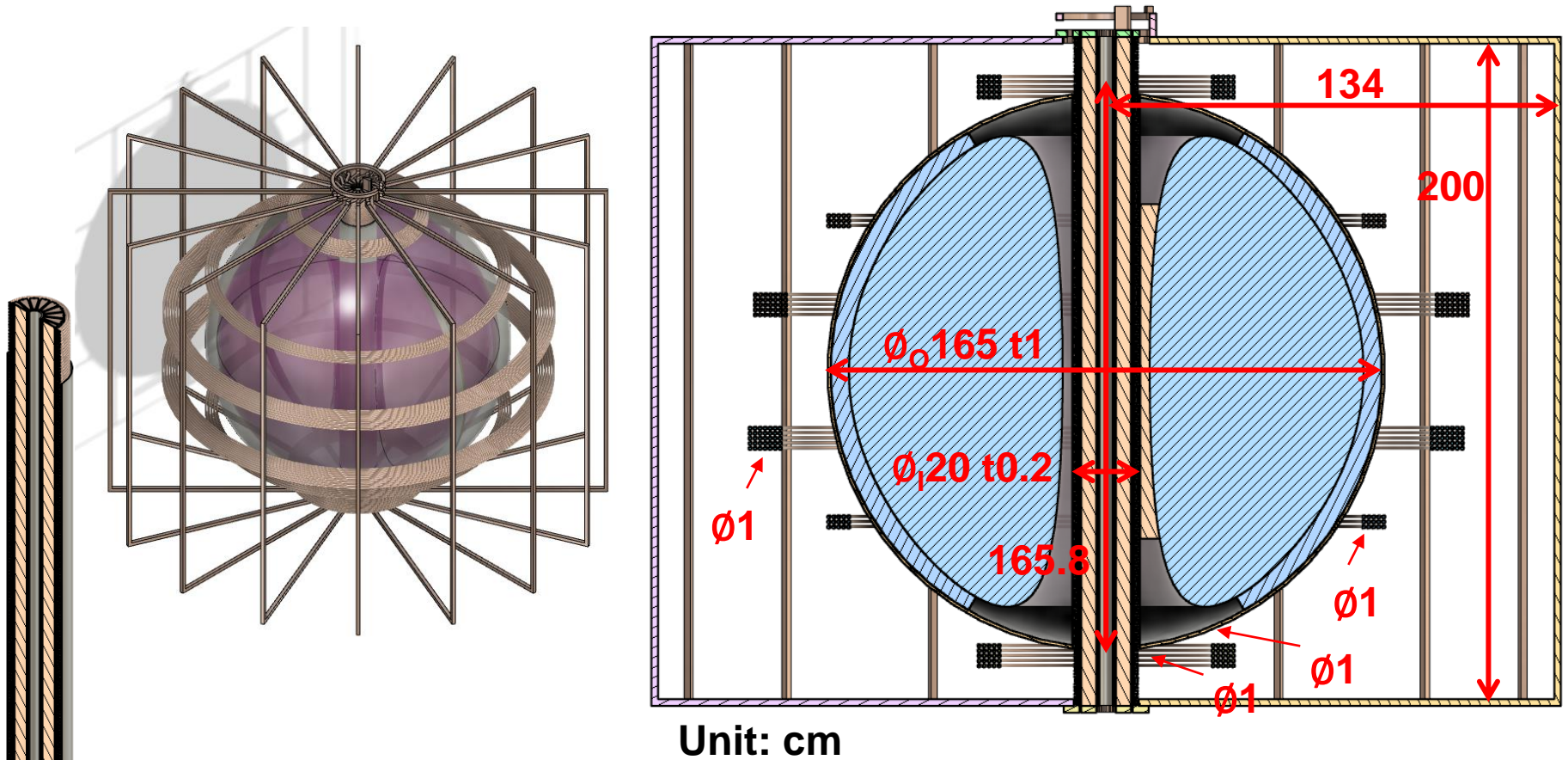
Poloidal coils are used to reduce the stray field during breakdown



• Currents of SMART

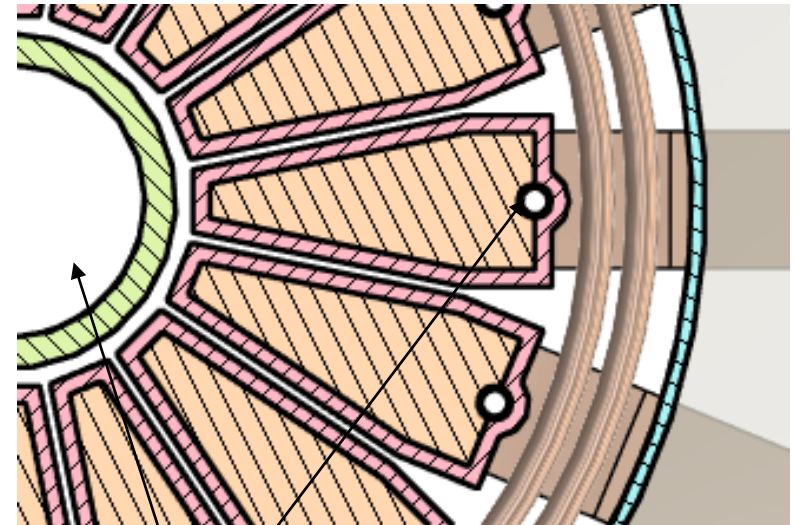
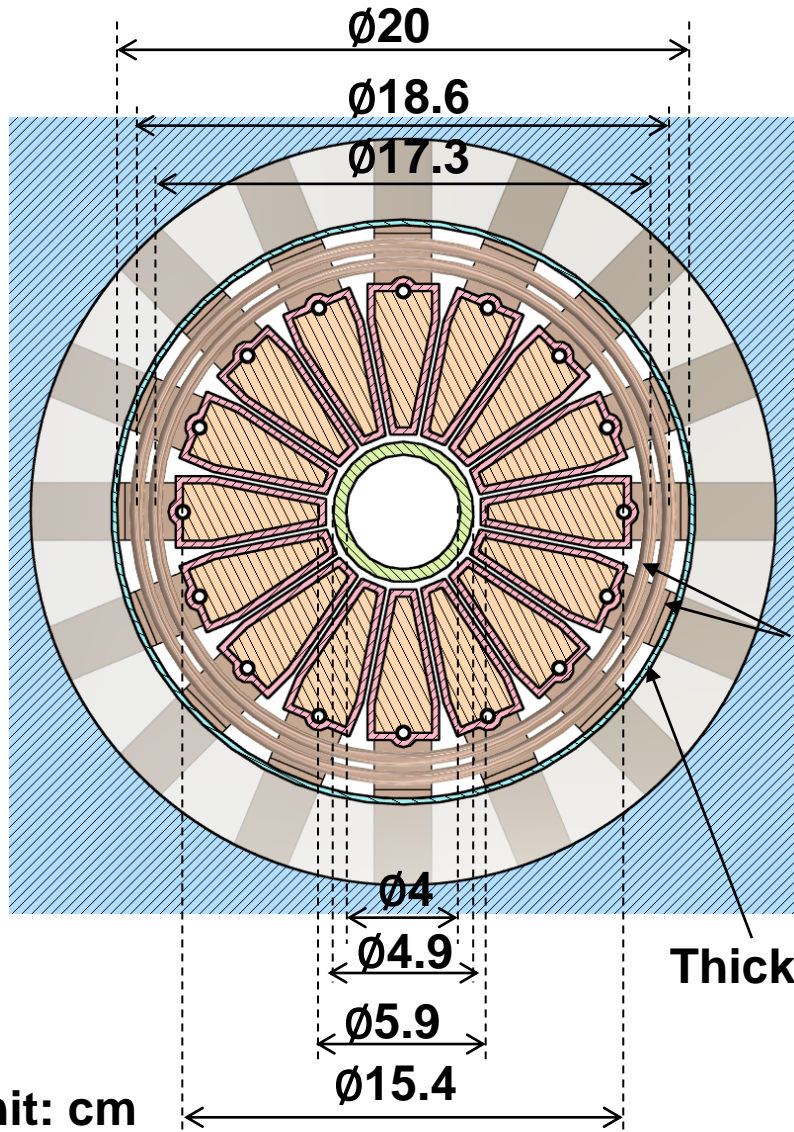


Potential design of Formosa Integrated Research Spherical Tokamak (FIRST)



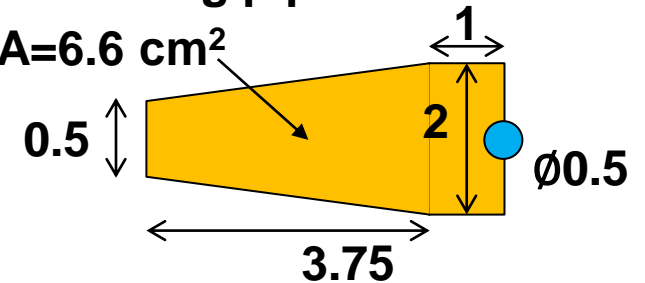
Central solenoid: $400=2 \times 200$ turns

There are limited space in the central stack for solenoid



For cooling pipe

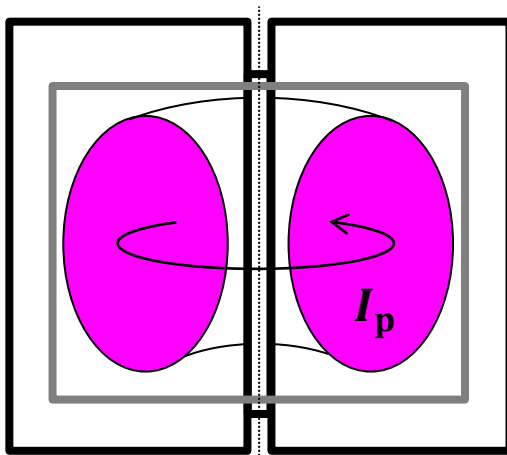
$$A = 6.6 \text{ cm}^2$$



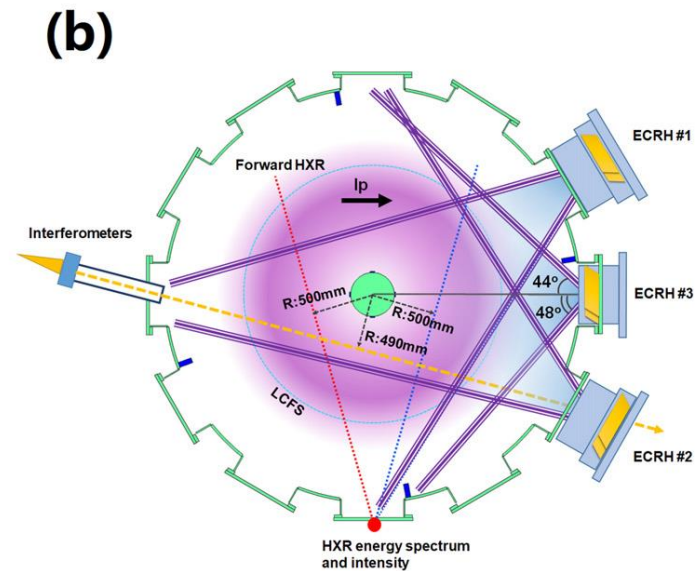
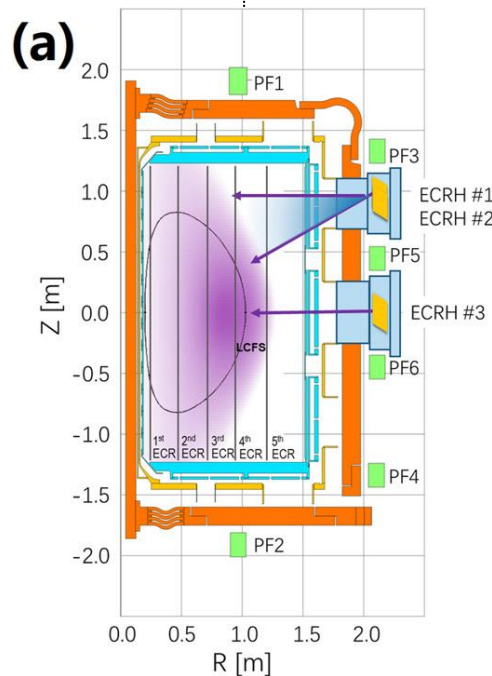
Unit: cm

- Temperature increase $\sim 80^\circ\text{C}$ for a current of 70 kA lasting 500 ms.

Momentum exchange may be needed to drive plasma current



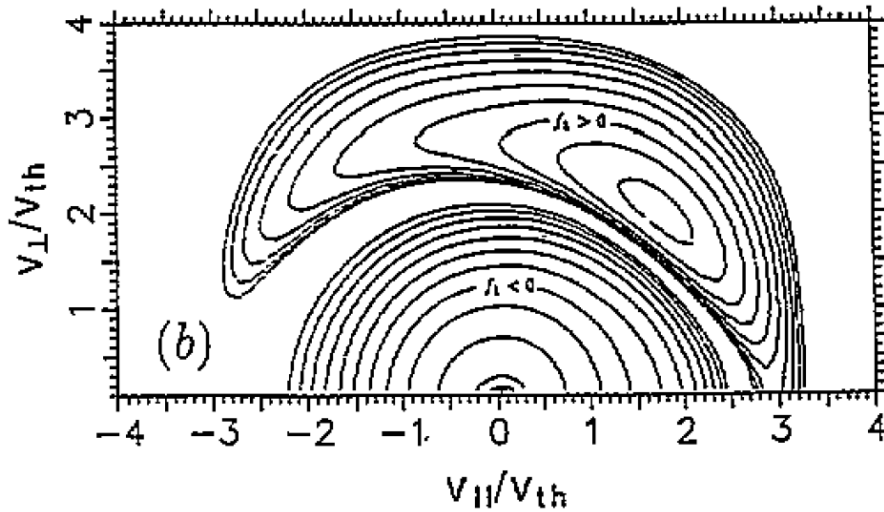
$$\vec{j}_p = \Sigma qn \vec{v} = -en_e \vec{v}_e + en_i \vec{v}_i$$



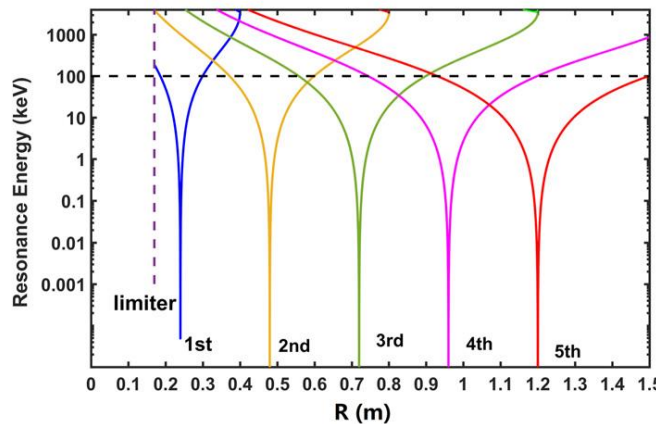
The collisional re-distribution of the ECRH-driven anisotropy in E_{\perp} causes some parallel momentum to flow from e^{-} to ions



- Coulomb collisions are more efficient at lower energies.

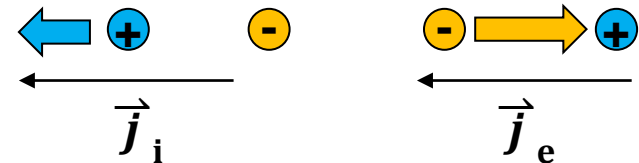


- Electron cyclotron current drive:



Velocity: $v_2 > v_1$

Collisions: $v_2 < v_1$



$$\vec{j}_p = -en_e \vec{v}_e + en_i \vec{v}_i$$

$$\vec{P} = n_e m_e \vec{v}_e + n_i m_i \vec{v}_i \approx 0$$

Temperature of 100 eV is the threshold of radiation barrier by impurities

